A thesis for the Degree of
Master of Engineering

Microwave Resonant Cavity Sensor for Liquid Identification

GRADUATE SCHOOL
JEJU NATIONAL UNIVERSITY

Department of Ocean System Engineering

Yoonsang Jeong

2021. 2.

Microwave Resonant Cavity Sensor for Liquid Identification

Yoonsang Jeong
(Supervised by professor Chong Hyun Lee)

A thesis submitted in partial fulfillment of the requirement for the degree of Master of Engineering

2021. 02.

This thesis has been examined and approved.

Jinho Bae

Thesis director, Jinho Bae, Dept. of Ocean System Engineering

Chong Hyun Lee

Chong Hyun Lee, Professor, Dept. of Ocean System Engineering

Yoon Hyeok Bae

Yoon Hyeok Bea, Professor, Dept. of Ocean System Engineering

2020. 12

Date

Department of Ocean System Engineering
GRADUATE SCHOOL
JEJU NATIONAL UNIVERSITY

ABSTRACT

RF Dielectric spectroscopy (DS) is a powerful monitoring technique that can quickly and accurately characterize the properties of various materials. Based on this principle, Radio frequency (RF)-based liquid detection and classification sensors have been widely studied in recent years and various RF-based sensors are being developed. In this thesis, we consider the problem of distinguishing liquids of similar electrical properties and propose two electromagnetic wave-based types cavity resonator sensor. The working principle of the proposed sensor is based on the fact that the change in permittivity of liquid samples inside cavity sensor will also cause a change in resonant frequency. The proposed resonator sensors consist of metal cavity that resonates according to the permittivity of liquid and a monopole that excites electromagnetic waves. For experiments, six different gasoline samples of permittivity in the range of 2.018 to 2.218. By using a gasoline permittivity of room temperature and changing sensor parameters, the sensors were designed by high-frequency structure simulator (HFSS). The designed sensors are cylindrical and rectangular type and have resonant frequencies of 7.119GHz and 5.13GHz for normal gasoline, respectively. The cylinder sensor is designed to distinguish the five gasoline samples, and the rectangular sensor to distinguish the six gasoline samples with additive new sample of permittivity difference of 0.016 with others. We obtain 8 MHz resonance separation sensor at room temperature to the sample of closest permittivity by the rectangular sensor experiments and 18 MHz by the cylindrical sensor experiments. To verify the feasibility of the fabricated sensors under temperature variation, experiments have been carried out using thermostatic chamber and vector network analyzer (VNA). The minimum frequency separation to distinguish gasoline samples of the

cylindrical sensor is found to be larger than 29 MHz with reflection coefficients under -11 dB when temperature changes from -35°C to 0°C. To verify the feasibility of the fabricated sensor under temperature variation from 0°C to 20°C by using the rectangular sensor, we derived a simple linear distinction function of resonance frequency and S11 parameter and we obtained a minimum 4.4MHz resonance separation by the function.

These results showed that the distinction performance for normal gasoline is robust to temperature variations. Through simulations we also showed that the distinction property is robust to design parameter errors, installation position variations and sensing time variations. These results show that the proposed sensor can be utilized effectively for distinguishing different DI gasoline.

TABLE OF CONTENTS

LIST OF FIGURES

LIST OF TABLES

1. INTRODUCTION

RF Dielectric spectroscopy (DS) is a powerful monitoring technique that can quickly and accurately characterize the properties of various materials. The DS works by extracting molecular characteristics of material under test (MUT) while it undergoes interaction with applied time-varying electric field over a broad frequency range [1]. The extracted information from the RF frequency regions is mainly comprised of permittivity (or dielectric constant), a frequency dependent property of the material that offers cost-effective, compact and simpler implementation of the sensing unit. Based on this principle, various RF-based sensors are being developed that measures the dielectric characteristics through the change in capacitance for each frequency represented by the S-parameter and resonant frequency. Using these parameters, classification, identification, and characteristic measurement of liquids are performed [2]. It is a potential research area for developing consumer and sensor based-electronics. Typically, it is used for monitoring the quality of food such as milk [3], measuring liquid flow conditions [4], glucose concentration in blood [5], salt water concentration [6] and sensing characteristics of chemicals such as ethanol [7-11].

Such a most studies focus on simple mixtures with relatively large differences in permittivity. By contrast, Research on RF sensors for complex blend material with small permittivity differences is insufficient. Therefore, in this paper, we proposed a cavity resonator sensor to distinguish liquids with small dielectric constant differences. The sample to be sensed issix diffrent DI gasoline samples inclusive sample of permittivity difference of 0.016.

Gasoline, also referred to as gasolene, is a complex blend of compounds of

volatile chemical constituents used as fuel for internal combustion engines [12]. It is well-known to automobile engineers that the volatility of gasoline plays a critical role in affecting vehicle drivability and operation [13]. The DI index is defined as the temperature at which specified fractions of the sample are distilled, and it is closely related to volatility. An appropriate drivability index leads to smooth acceleration, ease in engine cold-start/warm-up operations and no or far less surge while driving. The vehicles that use different blends of gasoline require some form of sensors to measure the DI and composition of the fuel. At present, different techniques have been used to measure the DI of fuel.

Lambert et. al. estimates the DI of the sample by heating a fuel sample placed between two narrow parallel plates of a capacitor and then measuring the change in capacitance of the sensing element as a function of time and temperature [14]. Another reported technique utilized platinum resistance temperature detectors (RTDs) to compare the engine exhaust gas temperatures during cold starts to actual engine exhaust air/fuel ratios using low and high DI fuels to detect the cold start volatility characteristic of the fuel [15]. The limitation to this technique is that it can not differentiate between various DI but only detect the presence of a HiDI fuel. Moreover, both of the techniques mentioned above generally require the sample to be heated for a substantial amount of time before the sensor becomes effective for control following a cold start. By contrast, RF techniques do not require the sample to be heated so quick measurements are possible.

Among microwave based designs, resonant cavities are easy to fabricate, require a minimal sample, possess excellent resonant characteristics that ensure higher accuracy [16], [17] and high sensitivity [18] when used explicitly in sensing resonant frequency locations. This attribute is useful for different material characterisation including nutrient monitoring in waste water treatment [19], food evaluation and analysis [20]. It is worth noting

that the resonant frequency is comparatively less sensitive to the impurities that increase the conductivity of fuel blends [21]. Many researches are based on cavity designs. Guo et. al. in [16] used cylindrical cavity opened at both ends for on-line water content measurement by measuring resonant frequency of the cylindrical cavity. Another reported sensor utilizes a cylindrical cavity for resonant frequency change between 5 and 5.7 GHz to analyze a two phase gas - liquid flow regime in a pipeline [22]. Ethanol content present in gasoline has a high permittivity that allows useful sensors to be built using relatively short lengths of metal enclosure cavities [21].

The as-developed sensor design is based on a rectangular metal cavity enclosure, which results in a small size and easy fabrication. The designed sensor was experimentally verified and demonstrated using an ANSYS high-frequency structure simulator (HFSS) and a vector network analyzer (VNA), which shows the consistency of the simulations with experiments. Additionally, the robustness of the sensor to temperature variations was also verified by conducting different experiments. The sensor shows an obvious change in resonance frequency with the change in DI, which can be effectively used for the distinction of different DI gasoline.

The content of the paper is organized as follows. Section 2 presents the cylindrical cavity sensor modeling and performance evaluation of the cylindrical cavity sensor, on the basis of simulation and experimental results, is discussed. Section 3 describes the rectangular cavity theory and sensor modeling along with an error analysis of the sensor via simulations and experiments and the sensor fabrication and experimental results, as well as a linear function for gasoline distinction, are described. In Section 4, the final conclusion of the paper is presented.

2. CYLINDRICAL CAVITY SENSOR

2.1. Sensor Modeling and Design

To distinguish between various gasolines, the proposed sensor model is shown in Figure 1. This sensor can be separated into two components: a monopole and a cylindrical cavity which can be built from circular waveguide by shorting metal walls at both ends. Figure 1(a) illustrates the geometrical structure of the cylindrical cavity resonator which consists of closed copper cylinder filled with sample of permittivity ε, where ε = ε0εr (ε0 is the permittivity of free space approximately equal to 8.85×10−12 F/m, and εr is the relative permittivity of the fuel). The proposed sensor design is chosen to be a closed metal cavity structure to avoid any external interaction since the sensor is to be used either inside the fuel tank or at the fuel inlet of the car where there is a chance of the presence of other electromagnetic waves. The interior of the cavity is a hollow uniform cylindrical shape. A small hole is kept at the top center of the cylindrical cavity for providing the feed source. The feed source is vertically placed into the cavity through the hole which acts as an intermediator from external equipment to the cavity for transmitting microwaves inside the metal enclosure and for monitoring its resonant behaviour. A monopole has been chosen as a feed source as shown in Figure 1(b). The degree of coupling is controlled by adjusting the length of the probe which is kept small to have minimum interaction with the field inside. The monopole is coated with thin layer of insulating medium Teflon to avoid direct contact with the testing gasoline samples in order to avoid corrosion which may lead the sensor to operate abnormally. Even though the current in the monopole is very small, an electric field is created between monopole and adjacent wall of the

resonator which is maximum at the location of monopole and also perpendicular to the wall. The current also generates a magnetic field that radiates like a magnetic dipole tangential to the wall.

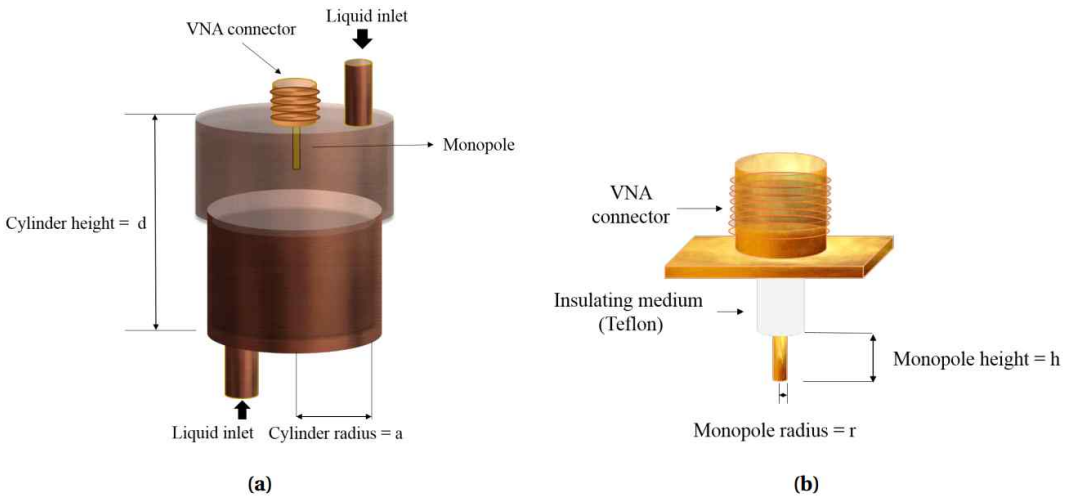

Figure 6. Geometrical structure of (a) Cylindrical cavity resonator (b) A coupling probe (monopole) fixed at the top center of cavity

The resonant frequency of the cavity exhibits a substantial change with a small change in square rootof permittivity ($\sqrt{\varepsilon}$) of gasoline samples. A basic experimental schematic utilizing the proposed sensor for measuring permittivity of different gasoline samples is shown in Figure 2.

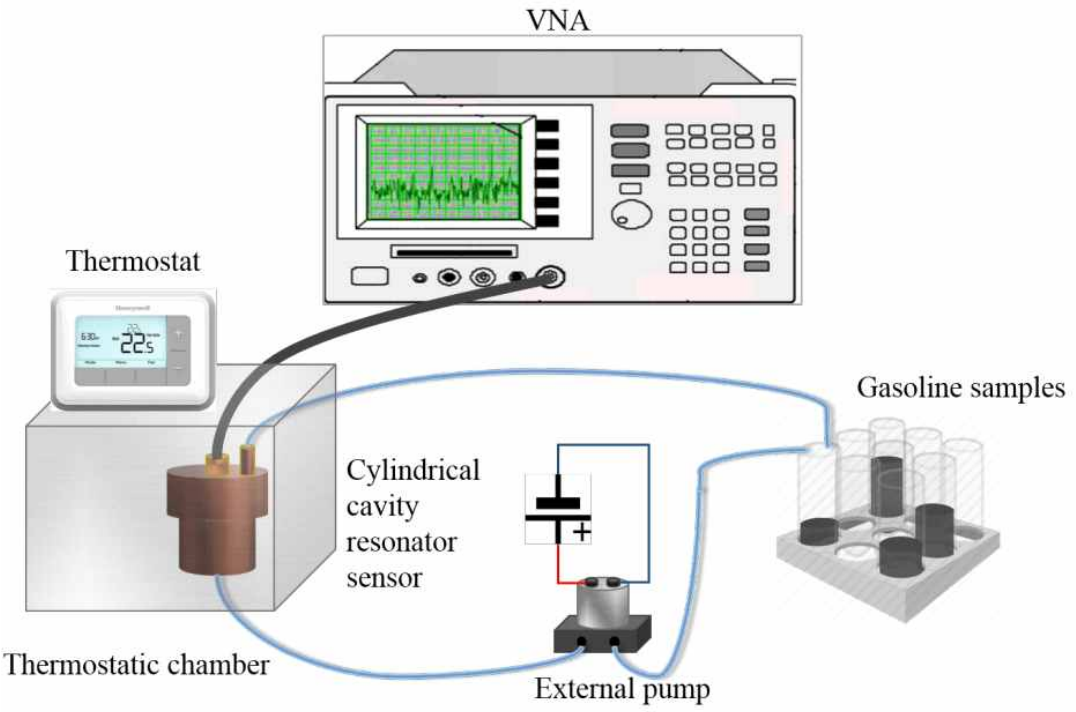

Figure 7. Experimental schematics of microwave cavity resonator for measuring permittivity of different gasoline samples

When resonance occurs, there is the possibility of the occurrence of various electromagnetic modes within a specific cavity where different modes have their own resonant frequencies, dimensions of cavities and associated Q-values [23]. The basic modes for cylindrical cavity resonators are transverse magnetic TM_{01} and transverse electric TE_{01} and TE_{11} [24]. In microwave theory, the higher-order mode decays rapidly, hence TM_{01}, the first higher mode of the circular waveguide, was selected. This selection was made since it is easier to manufacture as compared to the TE mode in actual application environment. In cylindrical cavity, the wavelength of the TM_{01} modecan be defined as [25]:

$$\lambda = 2.612a \qquad (1)$$

where a is the internal radius of the cavity. The resonant frequency for a given mode is calculated using Equation (2), where fnmt is the resonant frequency of the TM_{nmt} mode; m, n and t are the number of full-wave patterns along the circumference, the number of half-wave patterns along the diameter and the number of half-wave along the height of the cylindrical cavity respectively; d is the height of the cavity; P_{nm} is the mth root of Bessel function of nth order. The values of P_{nm} are listed in Table 1; c = 299792458m/s is the speed of light; μ_r is the relative permeability (value considered to be 1 since the gasoline samples are non-magnetic in nature) and ε_r is relative permittivity of the filled material inside the cylindrical cavity sensor.

$$f_{mnt} = \frac{c}{2\pi\sqrt{u_r\epsilon_r}}\sqrt{\left(\frac{P_{nm}}{a}\right)^2+\left(\frac{t\pi}{d}\right)^2} \qquad (2)$$

From Equation (2), it can be noticed that the utilization of higher frequencies may lead to small size cavities that in turn need a much lower quantity of the sample.

Table 1. The roots (Pnm) of the Bessel function

n \ m	1	2	3
0	2.405	5.520	8.654
1	3.832	7.016	10.174
2	5.135	8.417	11.620

2.2. Simulations Results of the Proposed Sensor

For transmitting and receiving electromagnetic waves, more than one antennas can be positioned inside the cavity. The most common arrangements are one-port or two-port cavities [26]. For one-port arrangement, when the testing material inside the cavity interacts with electromagnetic waves, a part of the power is reflected back which is termed the reflection coefficient or the return loss that can be measured with the help of VNA. This measure is used in the following simulations and experiments to analyze the performance of the proposed sensor. For sensitivity analysis, resonant frequency separation is chosen for the distinction of gasoline samples.

The proposed sensor is designed to attain wide frequency separations and low reflection coefficients for all scenarios. The design steps of proposed cavity sensor are as follows:

1) Selection of permittivity (ε): First, we selected the permittivity of gasoline for simulating the sensor model. The gasoline samples used in our experiments are high driveablity index (HiDI) samples with average permittivity value of 2.1 and the permittivity of normal gasoline used in the design of this sensor is 2.15, which is similar to the average permittivity of HiDI gasoline.

2) Selection of the cylindrical cavity mode and design frequency: The procedure of selecting TM012 and the design frequency is already described in Section 2.1.

3) Selection of cylindrical height (d): We have chosen the height of the cylindrical cavity through simulations by sweeping it for the frequency range of 6.7-7.7 GHz. Figure 3(a) shows the optimization process of selecting the cylinder height. It is chosen to be 35 mm as it gives the minimum reflection coefficient for the given frequency range.

4) Selection of monopole height (h): To find the best height for the design, we have observed that the height of 8 mm of monopole gives good response in terms of lower reflection coefficient as shown in Figure 3(b).

Similarly, all those optimized parameters were chosen as they gave the best results in frequency separations and reflection coefficients.

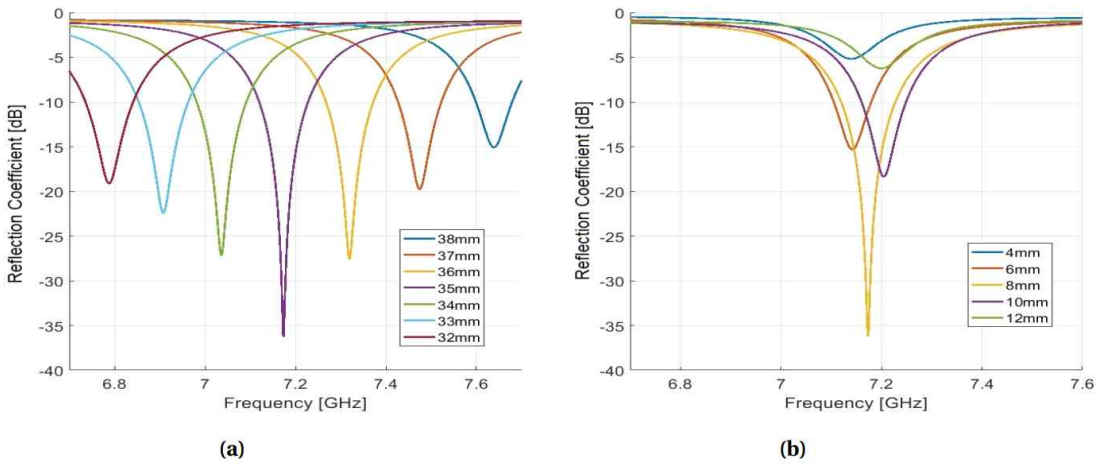

Figure 8. (a) Simulation results for the optimization of cylindrical cavity height (d) (b) Simulation results for the optimization of monopole height (h)

The proposed cylindrical cavity sensor is fabricated using conductive copper cylinder of inner radius (a) 19.2 mm and height (d) 35 mm. The manufactured sensor is shown in Figure 4(a). In this model, a coupling probe of height h and radius r is designed by extending the feeding coaxial cable with a small distance into the cylindrical cavity sensor and fixing at the bottom center. In our case, the height h of the probe is set to 8mm which is equal to one quarter of the wavelength of frequency 7.119 GHz making the input impedance nearly equivalent to that of an open circuit. The dimensions of coupling probe are 0.5mm × 8mm and it is wrapped with Teflon with radius size of 3mm as shown in Figure 4(b). The selected design parameters for the cavity resonator with height of 35 mm, radius of 19.2 mm and feeding height of 8mm showed minimum reflection coefficient

and largest frequency separation. The optimized parameters for the designed sensor are given in Table 2.

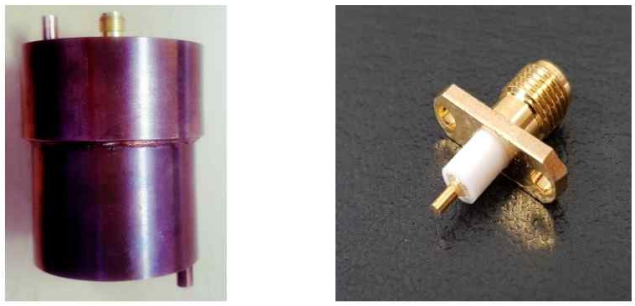

(a) (b)

Figure 9. (a) Actual fabricated sensor (b) Coupling Probe (Monopole)

Table 2. Design parameters of the proposed sensor

Parameter	Dimension (mm)	Parameter	Value
a	19.2	P01	2.405
d	35	t	2
h	8	Permittivity (ε)	2.15
r	0.5	mode	TM

The electromagnetic field of cylindrical cavity sensor with TM_{012} mode is simulated using HFSS software in Figure 5(a) and 5(b). It can be observed from these figures that the magnetic field of the TM mode is parallel to the cavity bottom and tangent to the wall of the cylinder and the electric field is perpendicular to both the magnetic field and the wall at the location of the probe. The intensity of electric and magnetic field is maximum at the center of the cavity and decreases approaching from the cavity center to the boundary. Therefore, these simulation results are in good agreement with theory in Section 2.1

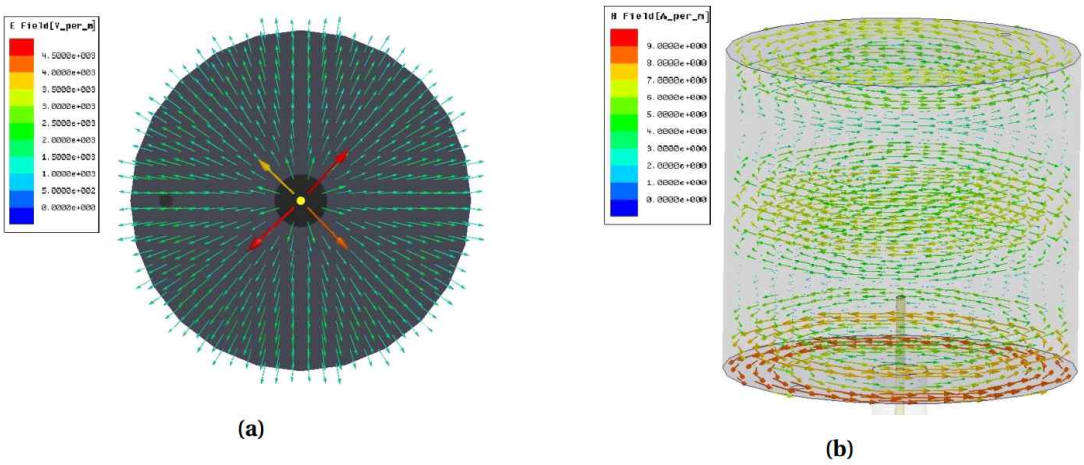

Figure 10. (a) Electric field top view of cylindrical resonator (b) Magnetic field side view of cylindrical resonator

By using HFSS, simulations have been conducted to analyze how the chosen design parameters and selected TM_{012} mode for the presented sensor affect reflection coefficients and frequency separation for different gasoline. We considered five different gasoline samples among samples specified in Table 3, which represents different types of standard gasoline/ethanol blends according to their ethanol content and emissions of nitrogen oxides (NOx), total hydrocarbon (THC), non-methane hydrocarbon (NMHC), carbon monoxide (CO). The reflection coefficients of the selected five samples of LEV3, Tier3, Euro4, Cold CO, Tier2 and one assumed sample (permittivity differ by 0.01 with LEV3) are shown in Figure 6 for a frequency range from 6.6 GHz to 7.7 GHz. Note that Euro4 of 2.134 permittivity has a high quality factor since it has closer permittivity to the designed permittivity 2.15. On the other hand, Tier3 of 2.289 permittivity has a low quality factor since its permittivity is not close to the designed value and has very small complex permittivity as compared to the other samples. The resonant frequency separation of four samples is greater than 100MHz and the reflection coefficients are below -12 dB. The minimum frequency separation of 18

MHz lies between the assumed sample and LEV3, which is still possible to distinguish.

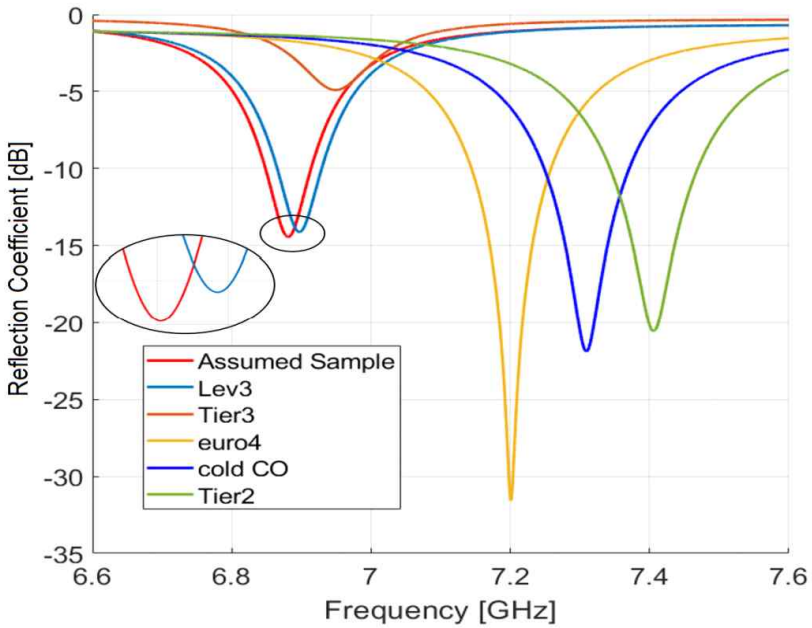

Figure 11. Simulation results of resonant frequency for the proposed sensor at 20 ○ C temperature for various gasoline samples

Table 3. Gasoline Samples according to emission standards for light vehicles, g/km [27],[28]

Index	Gasoline Samples	CO	THC	NMHC	NOx	Etanol (vol.%)
1	Tier 2 (Indolene)	3.5	-	2.16	4.44	<10
2	Tier 3 (Indolene E10)	3.5	-	-	4.9	14.8-15.2
3	LEV 2 (Phase 2)	6.4	0.032	-	0.05	<10
4	LEV 3 (Phase2 E10)	-	-	-	0.07	9.75-10.25
5	Cold CO	1.7	0.45	-	0.17	<10
6	Cold CO E10	1.5	0.4	-	0.2	10
7	Euro 4	1	0.10	-	0.08	<10
8	Euro 5	1	0.1	0.068	0.06	<10

Next, we simulated three different fuels such as kerosene, gasoline and heavy oil as mentioned in Table 4 to verify the resonance performance of the proposed sensor. The reflection coefficient according to frequency is shown in Figure 7. The response is plotted for a frequency range of 6 GHz to 8.5 GHz. Note that the proposed sensor exhibits remarkable resonant frequency separation between different fuel samples and has low reflection coefficients below -31 dB. Also, it can be easily observed that the resonant frequency has a negative relationship with permittivity.

Table 4. Simulation results of proposed sensor showing resonant frequency, reflection coefficient and permittivity for kerosene, gasoline and heavy oils [29] at room temperature (20°C)

	Kerosene	Gasoline	Heavy Oil
fr (GHz)	7.847	7.173	6.519
Γ (dB)	-31.5	-36.2	-32.0
ε	1.8	2.15	2.6

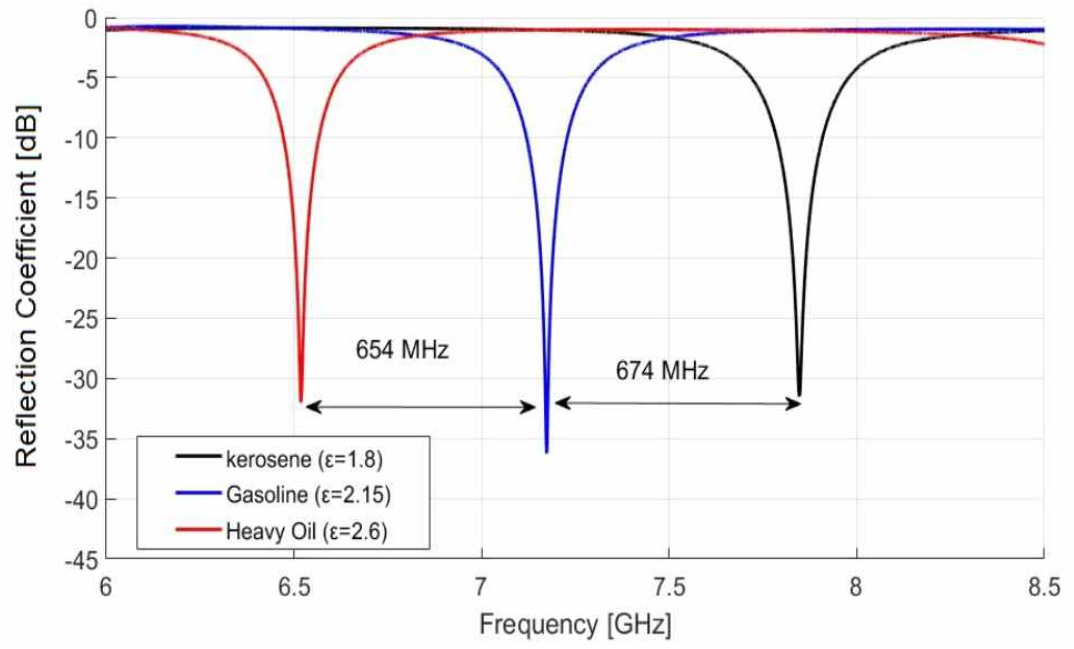

Figure 12. Reflection coefficient versus resonant frequency of the proposed sensor for kerosene, gasoline and heavy oils at room temperature (20 ○ C).

2.3. Experimental Results and Discussions

2.3.1. Experimental Setup

The experimental setup consisted of a cylindrical cavity resonator with monopole, VNA, external pump, thermostatic bathing, cable, capillary tubes and gasoline samples. The cylindrical cavity sensor is connected through a connector to supply microwave signals and to allow measurements to be taken using a calibrated series network analyzer VNA (100 KHz – 8.5 GHz E5063A, KEYSIGHT) via a 50 Ω coaxial cable. The gasoline solutions are introduced in the cavity via a thermoplastic capillary. In particular, the capillary is connected to an external pump via tube fittings so that a continuous gasoline flow is created and no air bubbles are formed in the capillary. A thermostatic bath and thermometer are used to control and monitor the temperature of gasoline samples as shown in Figure 8b. The experimental setup described above is shown in Figure 8a with gasoline bottles with different permittivities and microwave cavity sensor.

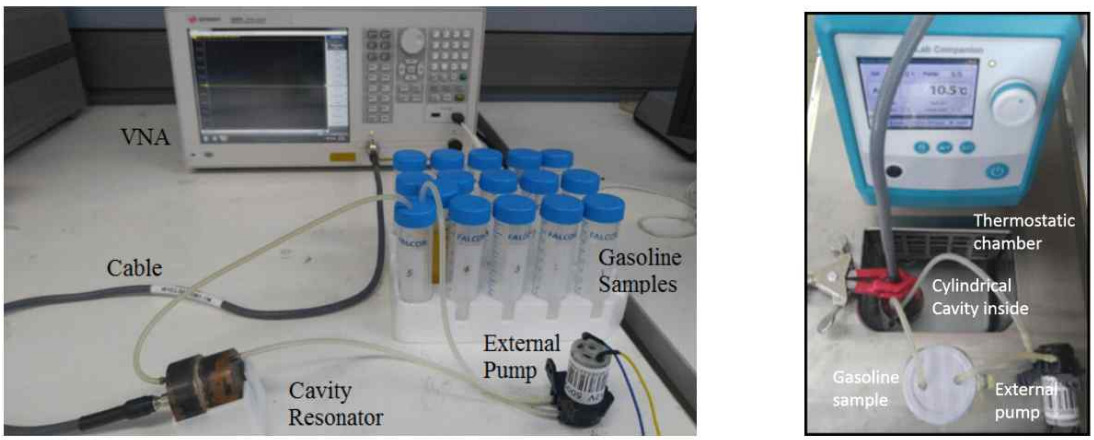

Figure 13. (a) Original experimental setup (b) Thermostatic bathing

2.3.2. Results and Discussion

Two important properties of dielectric materials are complex permittivity $\varepsilon^* = \varepsilon - j\varepsilon''$ and loss tangent $\tan\delta = \frac{\varepsilon''}{\varepsilon}$. The real part ε of ε^* is the permittivity (i.e. product of the free space permittivity ε_0 and the relative real/absolute permittivity ε_r) quantifying the stored energy within the medium and the imaginary part ε'' represents dielectric loss factor related to the dissipation of energy within the medium. The ratio tanδ quantifies the loss of power due to the propagation in a conductor. To analyze this loss of power, we performed experiments with the proposed sensor on gasoline samples with different permittivities as shown in Figure 9 using Table 5. The complex permittivity values were measured using N1501A permittivity measuring kit. The temperature of 20°C was chosen since the proposed sensor is designed at the same temperature and also the N1501A kit can measure permittivity only from 0 to 120 degrees.

Table 5. Real permittivity and measured complex permittivity for different gasoline samples at 20°C

Gasoline Sample	Permittivity Real (ε)	Permittivity Complex (ε'')
Tier2	2.018	0.0764
Cold CO	2.072	0.073
Euro4	2.134	0.066
Normal gasoline	2.15	0.0494
Tier3	2.289	0.0087
LEV3	2.324	0.0385

As we know that the permittivity of a solution changes with change in temperature, which in turn changes the resonant frequency. However, the effects are relatively small for hydrocarbon lubrication oils. The typical

decrease in permittivity for hydrocarbon oils is about 0.0013 to 0.05 percent per degree Celsius[30]. To verify this relationship and to analyze the ability of the proposed sensor for various gasoline samples in cold condition, we evaluated the sensor response as shown in Figure 10. The temperature range of 0°C to -35°C was chosen for the cold condition and the measurements were made with the help of thermostatic bath. In Figure 10, small and linear change in resonant frequencies according to the temperature variation can be observed. The minimum frequency separation of 31 MHz lies between Euro4 and Cold CO at 0°C temperature. The resonant frequency shifts towards a slightly higher value with the rise in temperature for Euro4, Cold CO and Tier2. For Tier3 and LEV3, the resonant frequency shifts slightly to a lower value since these two gasoline samples have higher percentages of ethanol and the ethanol tends to have low permittivity at higher temperatures[31]. Nonetheless, the performance of the proposed sensor is almost the same which confirms the robustness of the sensor with temperature changes.

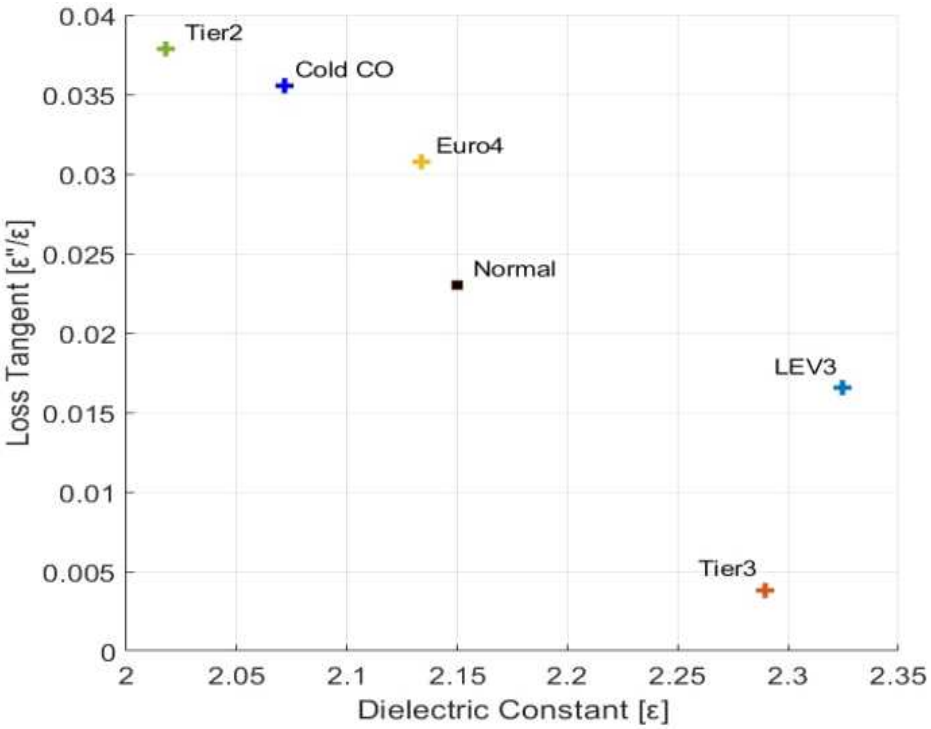

Figure 14. Variation of Loss-tangent(tanδ) with permittivity(ε) for different gasoline samples

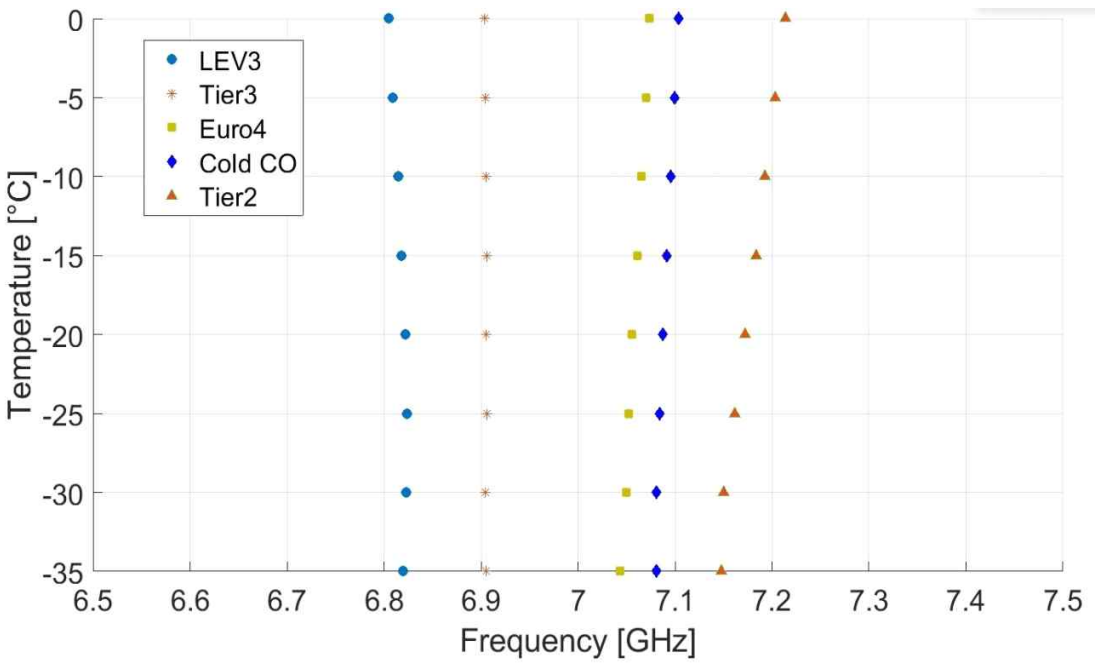

Figure 15. Experimental results of resonant frequency for the proposed sensor at different temperature for various gasoline samples

Using optimized parameters, we performed full wave analysis of the proposed sensor using HFSS for the frequency range of 6.5 GHz to 7.5 GHz under different temperature conditions. By sweeping frequency from 6.5 GHz to 7.5 GHz, we achieved reflection coefficient for LEV3, Tier3, Euro4, Cold CO and Tier2 at -35°C to 0°C temperatures as shown in Figure 11(a) and 11(b) respectively. The proposed sensor fulfills the requirement of large frequency separations between different samples making it sensitive towards small changes in permittivity of a given sample. The gasoline sample, Tier2 shows minimum reflection coefficient at -35°C with -63.64 dB dip at a resonant frequency of 7.15 GHz. In Table 6, the frequency separations of close resonant peaks are listed. At higher temperatures, the resonant frequency increases. Higher temperatures increase the activity of electrons and reduce the relative permittivity of fuels thus, resonant frequency as well as reflection coefficient increases. Here, the point to be noted is that the fuel with lower permittivity has higher resonant frequency and vice versa i.e. Tier2 as the fuel with the lower permittivity and LEV3 as the fuel with higher permittivity. These results reveal that the proposed cylindrical cavity sensor is still very sensitive to distinguish normal and HiDI gasoline under different temperature conditions.

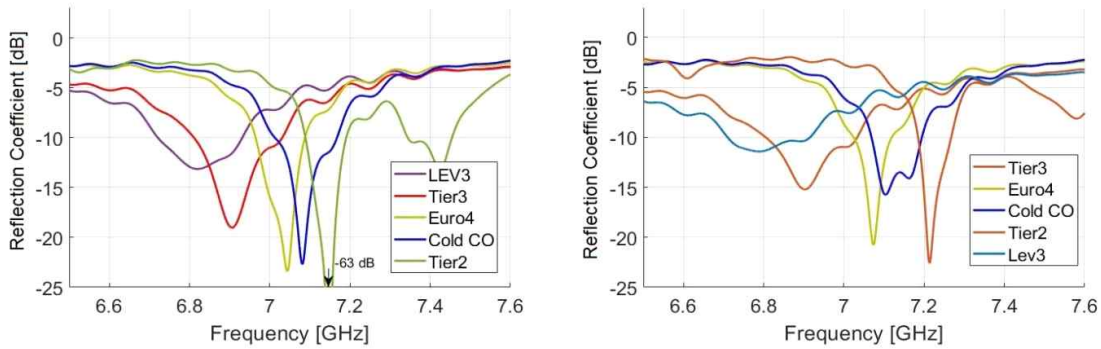

Figure 16. Reflection coefficient analysis of the proposed sensor at temperature (a) -35 ○ C (b) 0 ○ C

Table 6. Real permittivity and measured complex permittivity for different gasoline samples at 20 ○ C

Gasoline Samples	Resonant frequency [GHz]	Reflection Coefficient [dB]	Frequency Separation [MHz]
LEV3 (-35 ○ C)	6.818	-13.14	86
Tier3 (-35 ○ C)	6.904	-19.02	
Euro4 (-35 ○ C)	7.042	-23.4	36
Cold CO (-35 ○ C)	7.078	-22.69	
LEV3 (0 ○ C)	6.791	-11.41	112
Tier3 (0 ○ C)	6.903	-15.21	
Euro4 (0 ○ C)	7.074	-13.36	29
Cold CO (0 ○ C)	7.103	-15.71	
Tier2 (-35 ○ C)	7.148	-63.64	-
Tier2 (0 ○ C)	7.215	-22.37	

The relationship between permittivity of the different gasoline samples and resonant frequency is shown in Figure 12a where curve 1 shows theoretical values and curve 2 shows experimental values. The resonant frequencies of theoretical data are slightly higher than experimental values. The qualitative analysis of Figure 12(a) suggests that resonant frequency decreases monotonically with increase in permittivity in both curves. The experimental results are in agreement with that of theoretical results. Now, to perform quantitative analysis of the given data we define percentage error as follows: Percentage Error = |Experimental values - Theoretical|/Experimental values × 100. Figure 12b represents the percentage error between the theoretical and experimental values of resonance frequencies for various gasoline samples with different permittivity. The overall error is below 1.7%, which confirms the accuracy of the proposed sensor.

All the measurements were repeated five times with the same sample and their average value was considered. Samples with different dielectric constants in experimental measurements show various quality factors.

However, since the repeated measurement error of all samples is 0.5 MHz, which is smaller than the minimum resonant frequency difference 29 MHz between samples, it is possible to distinguish between different samples even considering LEV3 with a lower quality factor.

At the end, we have performed a comparison of our proposed method with the capacitor method, which is one of the DI measurement method presented in [14]. The results are summarized in Table 7. The sensitivities of the proposed sensor are achieved by taking the ratio of difference in resonant frequencies (f_r) of the samples to the difference in DI values and listed in Table 7 RF. Similarly, sensitivities of the sensor in [14] calculated by taking the ratio of voltage difference of the samples to the difference in DI values and listed in Table 7 Capacitor. It can be seen that the proposed sensor is better in terms of sensitivity to DI.

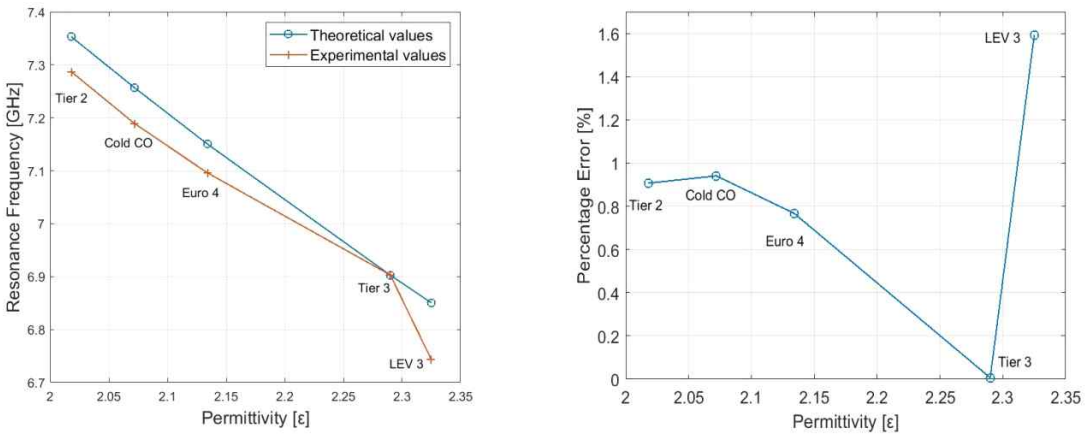

Figure 17. (a)Theoretical and experimental results of the proposed sensor for different gasoline samples at 20 ○ C temperature. (b) Percentage error between the theoretical and experimental results of the proposed sensor for different gasoline samples at 20 ○ C temperature.

Table 7. Sensitivity/DI the proposed RF method and capacitor method

Method	Sample	DI	Resonant Frequency fr [MHz]	Sensitivity [100KHz/DI]
RF	Cold CO	1132	7191.0	51.05
	Tier3	1075	6900.0	-
	LEV3	1168	6788.9	11.93
Capacitor	A	1131	2180	0.020
	B	1087	2090	-
	C	1164	2230	0.018

3. RECTANGULAR CAVITY SENSOR

3.1. Sensor Modeling and Design

3.1.1. Theory and Principle of Operation

The operating principle of microwave-based sensors depends on the interaction of electromagnetic (EM) waves with the material under analysis. Due to this interaction, the test material alters the signal velocity, causing reflection or attenuation. One of the main advantages of such sensors is their ability to safely measure in an enclosure without any external interaction using only EM penetrating waves. When the cavity is excited with an appropriate frequency, it starts to resonate, causing different resonance modes to occur. These resonance mode frequencies depend on the structural parameters of the resonator cavity and the dielectric properties of the sample inside. In a rectangular waveguide, TEM mode cannot occur, and the only propagating modes are TE and TM, in which the resonant frequency can be calculated using Equation (3) [32].

$$f_{mnt} = \frac{c}{2\pi\sqrt{u_r\epsilon_r}}\sqrt{\left(\frac{m}{a}\right)^2+\left(\frac{n}{b}\right)^2+\left(\frac{l}{d}\right)^2} \qquad (3)$$

where m, n, l are the mode numbers; c is the speed of light; μ_r denotes the relative permeability (since the gasoline samples are nonmagnetic, the value is taken to be 1); ϵ_r is the relative permittivity of the sample and a, b, c are the width, height and depth of the cavity, respectively. For TM modes, the values $m = n = 0$ are not a possible combination; therefore, the lowest frequency mode with stable resonant frequency for the rectangular

cavity is TM_{110}. It is desirable to have a maximum intensity of the magnetic field and minimum intensity of the electric field where the sample is present.

A higher magnetic field results in effective excitation and an increased signal-to-noise ratio (SNR), while a higher electric field deposits higher power, which leads to sample heating. The condition is further worsened if the sample is conductive [32].

The Q value of the cavity sensor can be largely defined as the loss Q_{mnl} due to the cavity wall and Q_{3dB} representing the sharpness of resonance. The loss Q_{mnl} due to the cavity wall of the rectangular cavity resonator operating in m, n, l mode is given in Equation (4).

$$Q_{mnl} = \frac{Z_W abc k_{xy}^2 k_{mnl}}{4R_s[b(a+d)k_x^2 + a(b+d)k_y^2]} \quad (4)$$

$$(k_x = m\frac{\pi}{a}, k_y = n\frac{\pi}{b}, k_z = l\frac{\pi}{d}, k_{xy} = \sqrt{k_x^2 + k_y^2}, k_{mnl} = \sqrt{k_x^2 + k_y^2 + k_z^2})$$

where Z_W is the natural impedance of air and R_s is the surface resistance of the resonator wall. The higher the Q_{mnl}, the more energy is stored in the cavity compared to the power consumed by the cavity wall [33]. The sharpness of resonance Q_{3dB} is as shown in Equation (5) [34].

$$Q_{3dB} = \frac{f_r}{B} \quad (5)$$

In this equation, f_r is the resonance frequency, and B is the bandwidth, which is the difference between the two frequencies that are 3 dB higher than the reflection loss of the resonance frequency. The higher the Q_{3dB} value, the lower the return loss and narrow bandwidth; therefore, it is easy to distinguish gasoline samples. In this paper, the process of optimizing the Q_{3dB} value of the sensor is performed through simulation during the design

of the sensor.

The designed sensor model is shown in Figure 13. The sensor is composed of two major components: a monopole and a rectangular cavity made up of copper enclosure filled with relative permittivity εr(ε=ε0εr,whereε 0andεarethepermittivitiesoffreespaceandgasoline,respectively). The interior of the rectangular cavity is hollow with a small feeding source vertically placed at the center for the transmission of EM waves. As described in (3), the cavity sensor exhibits a specific resonance mode according to the design parameters and sample permittivity. A thin protective layer of insulating medium is coated over the monopole to avoid corrosion and direct contact with the samples inside, which may cause unwanted results.

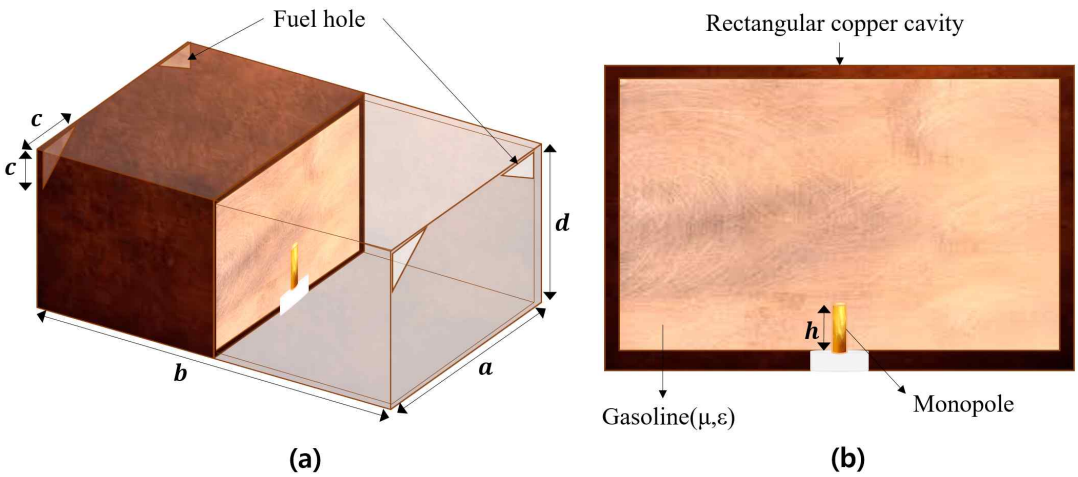

Figure 18. Geometry of the proposed sensor. (a) Isometric view, (b) Side view.

3.1.2. Sensor Design and Simulation Results

By using HFSS, the proposed sensor is designed to detect normal gasoline among various gasolines, including HiDI gasolines. The sensor is designed for commercialization and has a resonance band below 6 GHz, which is common operating frequency of commercial RF device. Moreover, the sensor is designed considering the characteristics of a rectangular resonator that increases the rate of change of the resonance frequency per relative permittivity and decreases the size of the sensor in the high frequency band, which is found to be 5~6 GHz. The simulation model for the design of the sensor is shown in Figure 14.

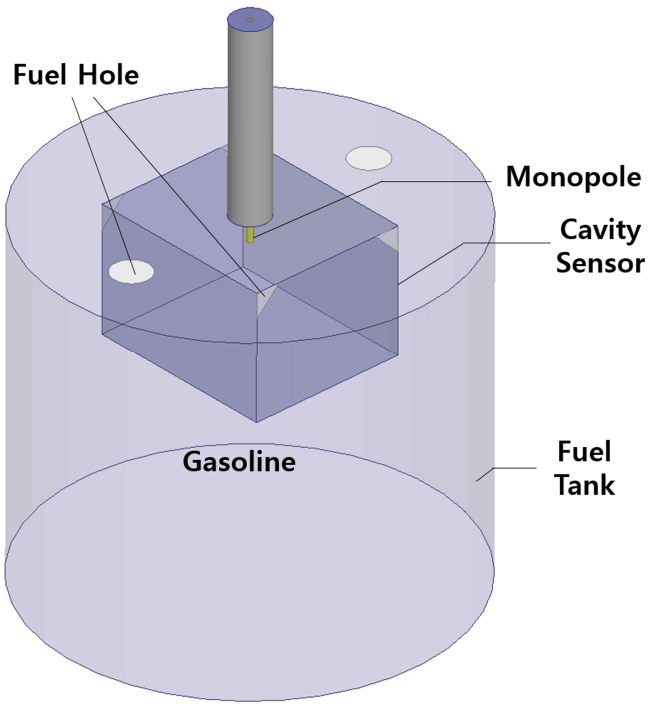

Figure 19. Simulation model

The sensor is modeled as a structure contained in a fuel tank filled with gasoline. The dimensions of the sensor are optimized to have a basic TM_{110} resonance with a high Q_{3dB} value for the previously mentioned resonant

frequency band. The design procedure of the proposed rectangular cavity sensor is as follows:

Enclosure width (a) and height (b): By setting the permittivity of normal gasoline to 2.157, the dimensions are designed to have a resonance frequency range from 5 GHz to 6 GHz. The dimensions are determined to have TM_{110} [23].

Enclosure depth (d): The frequency responses according to various depths are evaluated to examine the Q_{3dB} at TM_{110}. The optimum depth (d) can be obtained as shown in Figure 15(a). Monopole height (h): Similar to step 2, the height of the monopole is optimized to have a high Q_{3dB} at TM_{110}. The simulation results are shown in Figure 15(b).

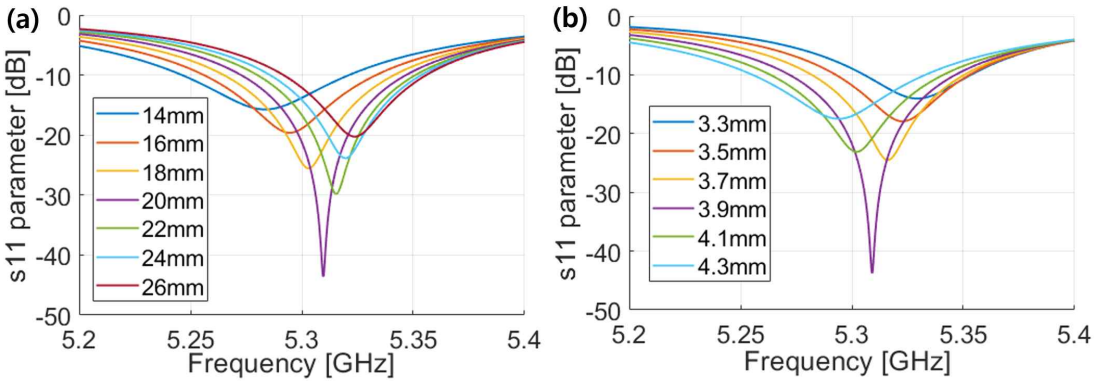

Figure 20. S11 parameters vs. (a) Sensor depth, d, (b) Monopole height, h.

The design parameters of the proposed cavity sensor are summarized in Table 8 The optimized width a, height b, and depth d, are set to be 30 mm, 25 mm and 20 mm, respectively. The monopole height h, is 3.9 mm, and e is the edge length of the triangular hole.

Table 8. Optimized Sensor Parameters

Parameter	Dimension (mm)	Parameter	Values
a	30	Mode	TM
b	25	Mode numbers (mnl)	110
d	20	Resonant Frequency band	5-6 GHz
h	3.9		
e	4	Permittivity (εr)	2-2.2

The designed sensor is verified by using HFSS software, as shown in Figure 16 and 17. It can be observed from Figure 16. that the EM field at resonance frequency matches well with the designed TM_{110}. Note that the magnetic field of the TM mode is perpendicular to the sensor depth direction, and the order of the electric field is one to the width and height directions.

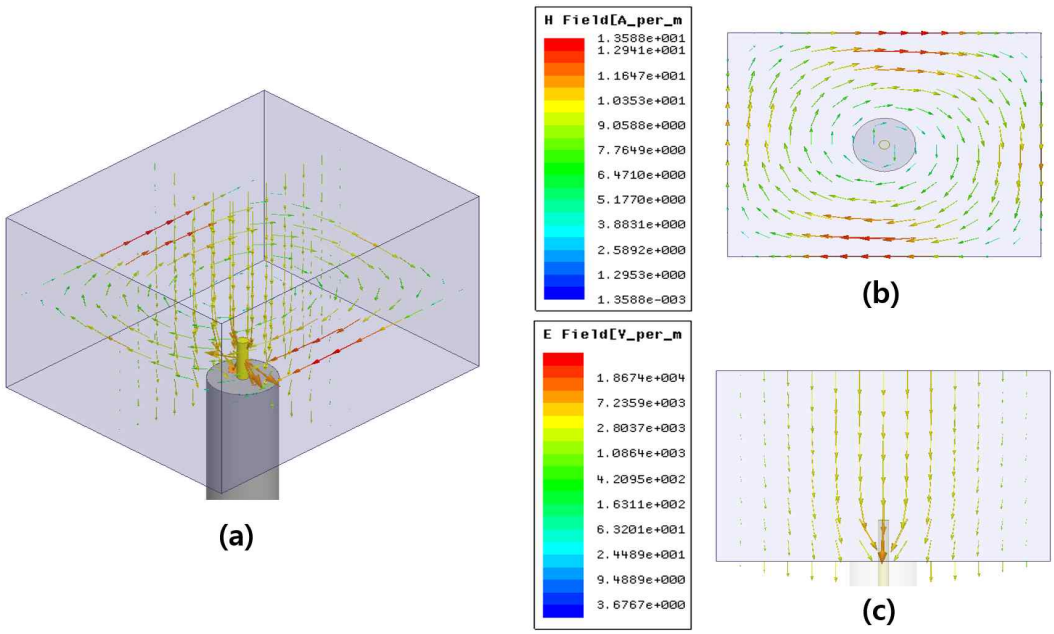

Figure 21. EM fields in TM110 mode.(a) EM field, (b) Top view of the M field, (c) Top view of the E field.

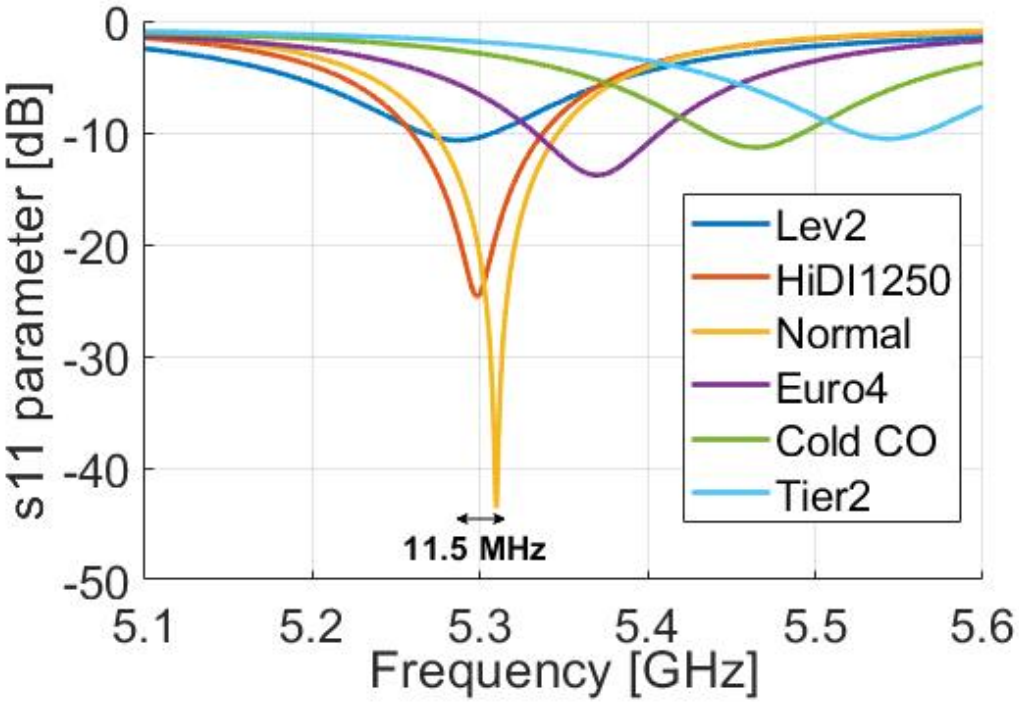

Figure 22. Frequency responses of normal and HiDI and gasolines with the designed sensor.

The frequency responses of the proposed sensor for HiDI and normal gasoline are plotted in Figure 17. The permittivities and the corresponding loss tangents are summarized in Table 9. These values are measured at room temperature (19°C~21°C) by using an N1501A permittivity measuring kit by KEYSIGNT Technology, and the average of 5 measurements taken from the measurement system is measured. The corresponding experimental environment for measuring the permittivity is shown in Figure 18.

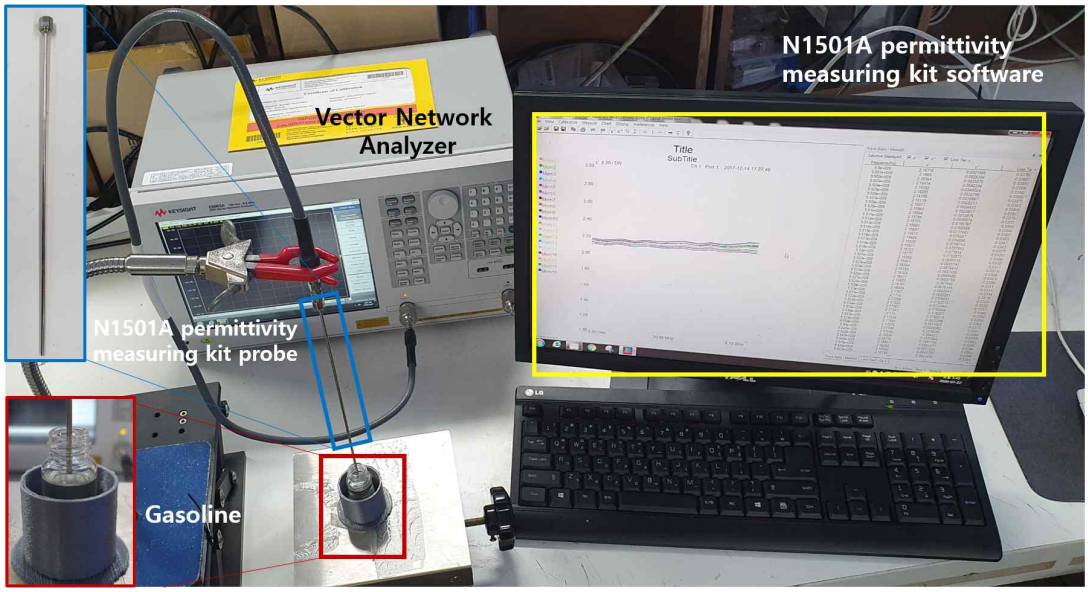

Figure 23. Setup for measuring permittivity at room temperature

Table 9. Units for Electric Properties

Gasoline	DI	Permittivity	Loss Tangent [ε”/ε]
Tier2	1144	2.018	0.038
Cold CO	1132	2.072	0.036
Euro4	N/A	2.134	0.031
Normal	443	2.157	0.02
HiiDI1250	1255	2.173	0.023
Lev2	1168	2.218	0.042

The minimum permittivity difference between normal and HiDI gasolines is as small as 0.016. Nevertheless, the resonance separation of the proposed sensor becomes at least 11.5 MHz, which is much higher than the 0.1 MHz frequency resolution of VNA. This large frequency margin, along with the high Q_{3dB} factor at normal gasoline resonance frequency show the validity of the proposed sensor plausible.

3.1.3. Sensitivity Analysis of the Sensor

To verify the reliability of the designed sensor, we conducted a few simulations by changing the design parameters.

1) Effect of sensor position on sensing property

To show that the resonant characteristics of the proposed sensor are robust to sensor positions, we consider a fuel tank of 45 L, which is full of normal gasoline. Next, we measure variations in resonance frequencies and S11 parameters by moving the sensor position by 50 mm. The obtained results are shown in Figure 19, in which the resonance frequency shift and S11 difference are less than 300 kHz and 4.01 dB, respectively. These numbers reflect less than 0.0056% changes in resonance frequency and 8% changes in S11 parameters, which are negligible changes for normal gasoline distinction.

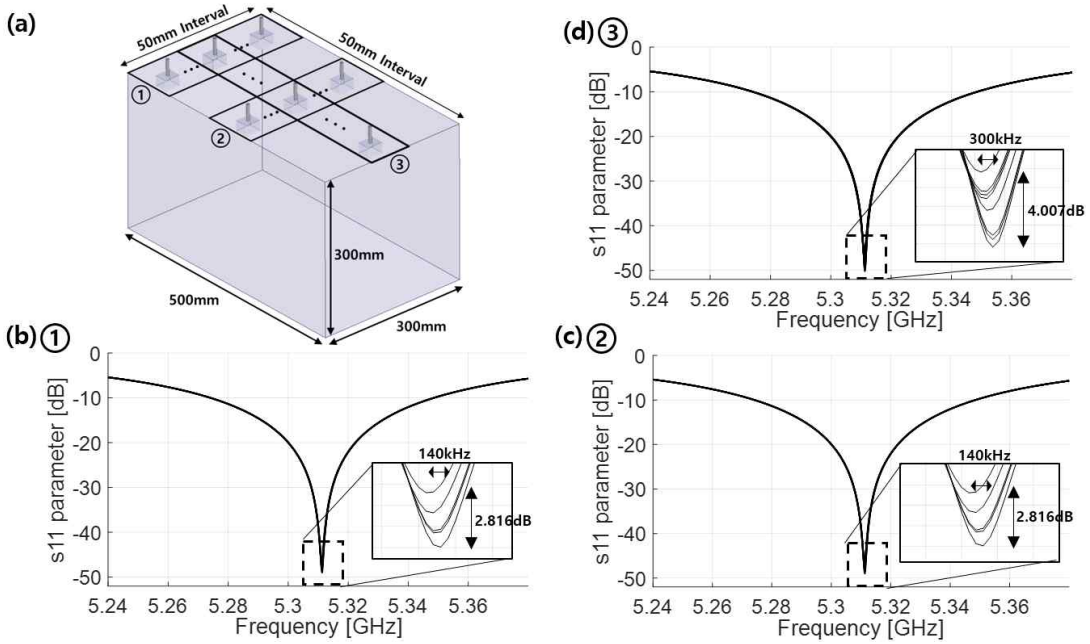

Figure 24. (a) Simulation setup, (b) Frequency responses at position①, (c) Frequency responses at position②, (d) Frequency responses at position③

2) Effect of sensor parameters on sensing property

To determine the reliability of the proposed sensor, we have investigated sensing performance by considering errors in parameters given in Table 8. In this study, we only consider one parameter at a time while the other three parameters are fixed as optimum values. To evaluate the sensing property, we only consider the closest sample HiDI1250, instead of all samples, because the rest of the HiDI samples are far more separated than the HiDI1250. To set the threshold of two sample separations, we choose a 10 MHz frequency separation and consider three S11 parameter values of -20 dB, -25 dB and -30 dB.

By changing a size from 20 to 30 mm in 0.05-mm increments, we obtain resonance responses and evaluate resonance separation and minimum S11 parameters according to a size, which are shown in Figure 20. Next, we obtain resonance responses and evaluate resonance separation and minimum S11 parameters according to b size, which are shown in Figure 21 by changing b size from 25 to 32 mm in 0.1-mm increments. Similarly, we obtain resonance separation and minimum S11 parameters according to d sizes of 0.5 mm increments and to h sizes of 0.02 mm increments and present them in Figure 22 and 23, respectively.

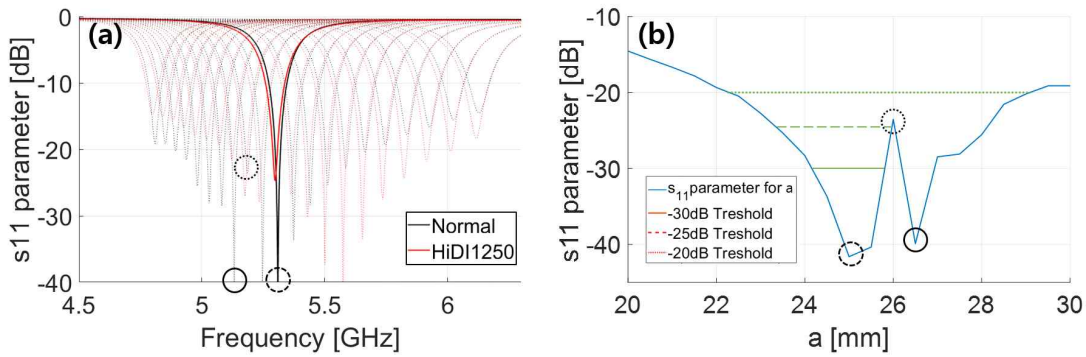

Figure 25. (a) Frequency responses according to size variations of a, (b) Minimum S11 vs. size variations of a

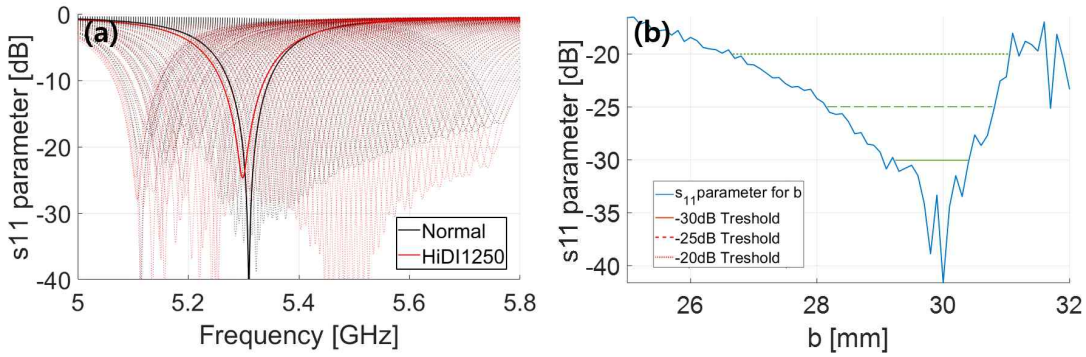

Figure 26. (a) Frequency responses according to size variations of b, (b) Minimum S11 vs. size variations of b

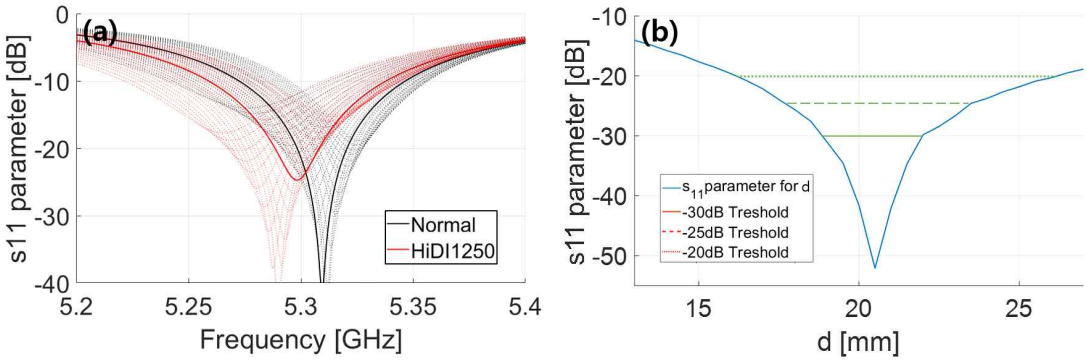

Figure 27. (a) Frequency responses according to size variations of d, (b) Minimum S11 vs. size variations of d

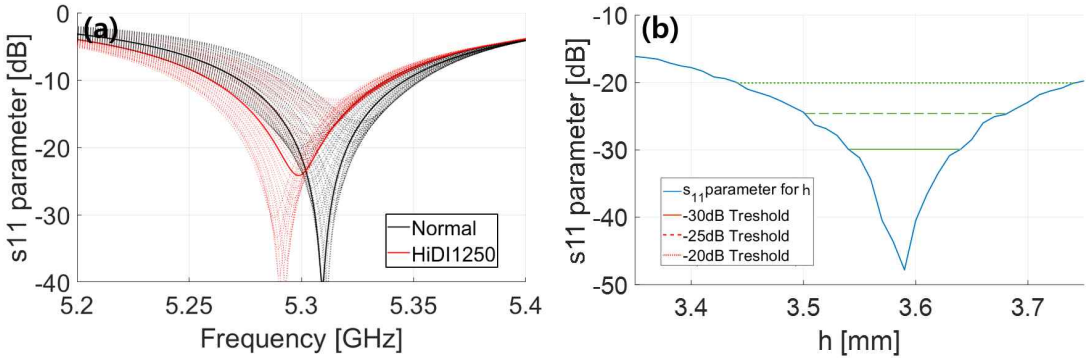

Figure 28. (a) Frequency responses according to size variations of h, (b) Minimum S11 vs. size variations of h

The tolerances of the a, b, d and h size errors according to the three S11 parameter thresholds are summarized in Table 10.

Table 10. Tolerance of Design Parameter Errors According to S11 Parameter Thresholds

Design Parameter [mm]	S11Threshold	-20 dB	-25 dB	-30 dB
a [25]	Δa [mm]	-2.5~4	-1.5~0.6	-0.75~0.5
	error [mm]/[%]	6.5/26	2.1/8.4	1.25/5
b [30]	Δb [mm]	-3.3~1	-1.8~0.8	-0.7~0.4
	error [mm]/[%]	4.3/14.3	2.6/8.7	1.1/3.7
c [20]	Δd [mm]	-3.5~6	-2~3	-1~1.9
	error [mm]/[%]	9.5/47.5	5/25	2.9/14.5
d [3.9]	Δh [mm]	-0.3~0.28	-0.18~0.14	-0.12~0.08
	error [mm]/[%]	0.58/14.9	0.32/8.2	0.2/5.1

The evaluated minimum design margin at -30 dB is 3.7% in b size, and the maximum is 14.5% in d size. The minimum and maximum design margins increase to 14.3% in b size and 47.5% in d size, respectively. Note that the minimum resonance separations under the a, b, d and h size errors are greater than the predefined 10 MHz threshold, as shown in Figure 24. These results prove that the proposed sensor design is a reliable fabrication method.

3) Effect of sensor parameters on resonance frequency

To check the stability (stable distinction) of the proposed sensor according to sensor size errors, we have investigated resonance frequencies of the closest sample HiDI1250 and normal gasoline. The frequency separations according to a, b, d and h size variations are shown in Figure 24. From the

figure, we can notice that the minimum 10 MHz separations are maintained at resonance frequencies for all considered design parameters. These results assure that the proposed sensor guarantees stable distinction of normal gasoline.

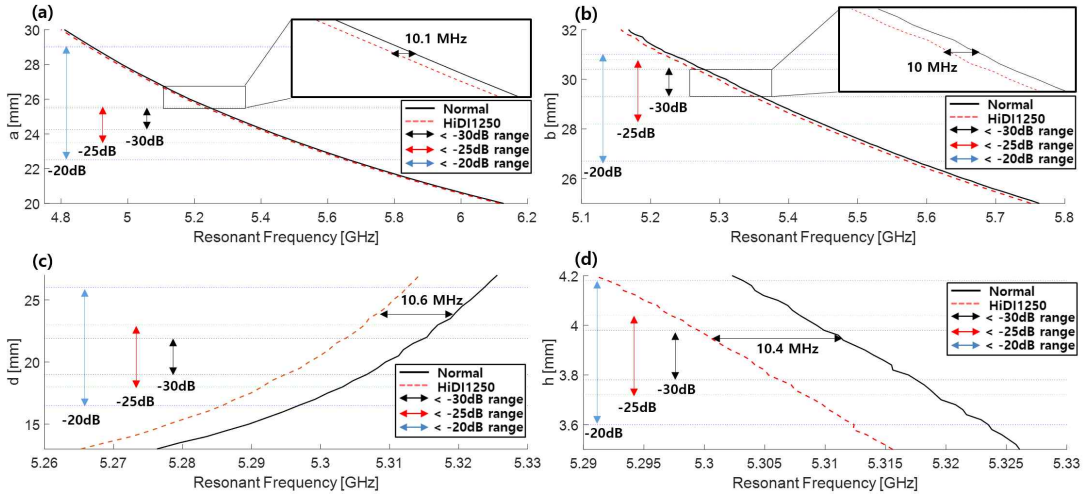

Figure 29. Resonance frequencies of normal and the closest HiDI vs. (a) size variations of a, (b) size variations of b, (c) size variations of d, (d) size variations of h

3.2. Experimental Results and Discussion

3.2.1. Sensor Fabrication and Verification

Based on the parameters in Section 3.1, we fabricate the proposed sensor, as shown in Figure 25. During the fabrication process, the length of the sensor monopole was adjusted from 3.9 to 3.7 mm to compensate the manufacturing error. The monopole of the sensor is fabricated using an SMA connector, and the enclosure is fabricated using a 0.3 mm copper plate. The sensor is attached to the top of the small aluminum fuel tank, in substitution for the car fuel tank. The tank is a cylindrical aluminum case with a size of 32 X 55 mm (radius X height) tightened to the sensor with a rubber ring. The gasoline is injected with a motor pump through the two circular fuel holes at the top of the tank until the sensor is sunk under gasoline. The gasoline reaches the sensor through triangular fuel holes with edge dimensions (e) of 4 mm.

Figure 30. Manufactured sensor and tank. (a) Monopole, (b) Rectangular Cavity Sensor enclosure, (c) Fuel Tank, (d) Assembled form.

The sensor is a shielded cavity sensor; therefore, theoretically, the fuel size does not affect the sensitivity of the sensor. To verify insensitivity, the simulation model and results with different fuel tank sizes are shown in

Figure 26. In simulations, three size of the fuel tanks are considered such as 32 X 55 mm (the proposed size), 64 X 110 mm (twice of the proposed size) and 150 X 450 mm (equivalent to 31.8 L fuel tank, 150^2 X π X 450 = 31,808,625 mm^3). The resonance frequency of the proposed sensor is 5.3074 GHz, and the reflection coefficient is -43.58 dB when the proposed 3255 mm fuel tank is considered. Note that the difference in resonance frequency and reflection coefficients for three fuel tanks is less than 1.7 MHz and 2.54 dB, respectively. These results show that the sensor performance is insensitive to the outside fuel tank size.

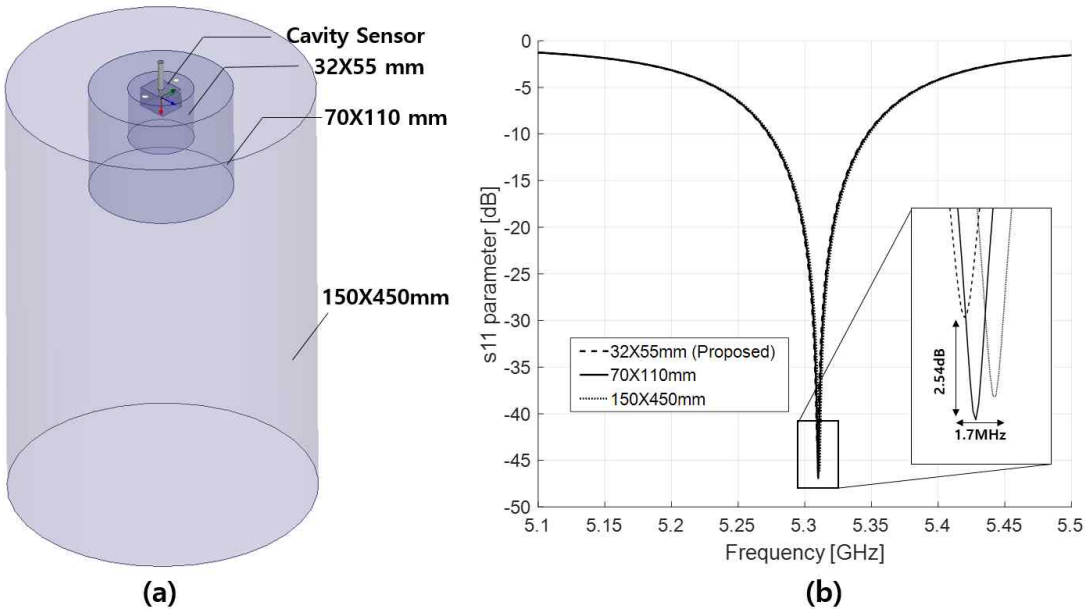

Figure 31. (a) Models of three fuel tanks, (b) Frequency responses of three fuel tanks.

The measured average frequency response of the fabricated sensor with S11 parameters according to various gasoline samples at room temperature (19℃~21℃) is shown in Figure 27. The S11 parameter for normal gasoline at resonance frequency increases from -36.7 dB to -26.9 dB, which it is still lower than other resonance frequencies of HiDI gasolines. The minimum

frequency separation among resonance frequencies of HiDI gasoline is measured as 8 MHz, which is sufficient for the distinction of HiDI gasolines. Additionally, note that the 8 MHz frequency margin can guarantee distinction of normal gasoline even when 0.1 MHz of max frequency deviation of five measurements is considered.

To verify the resonance frequency relation with permittivity, as given in Equation (3), HFSS simulation and experiments were performed at room temperature. The resonance changes are displayed in Figure 28, which shows that the measurements decrease as permittivity increases. The 39 MHz of average resonance frequency deviation from the simulations can be explained by experimental and fabrication errors. Nevertheless, we can observe that the proposed sensor exhibits remarkable resonance frequency to unity permittivity ratio as 931 MHz/ε by computing the slope of the dotted measurement fitting line.

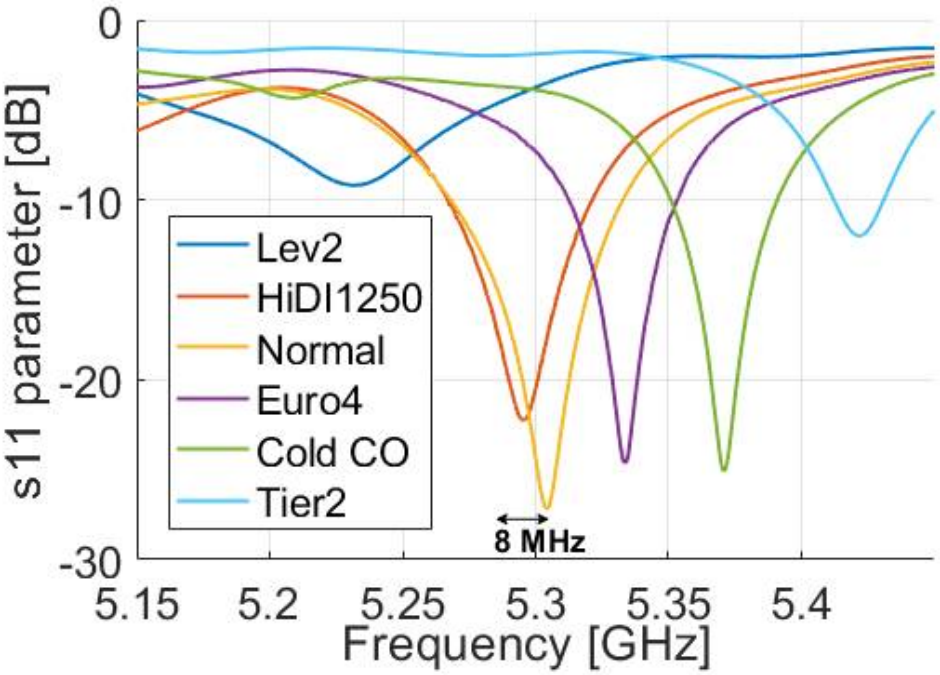

Figure 32. Frequency responses of normal and HiDI gasolines with the fabricated sensor

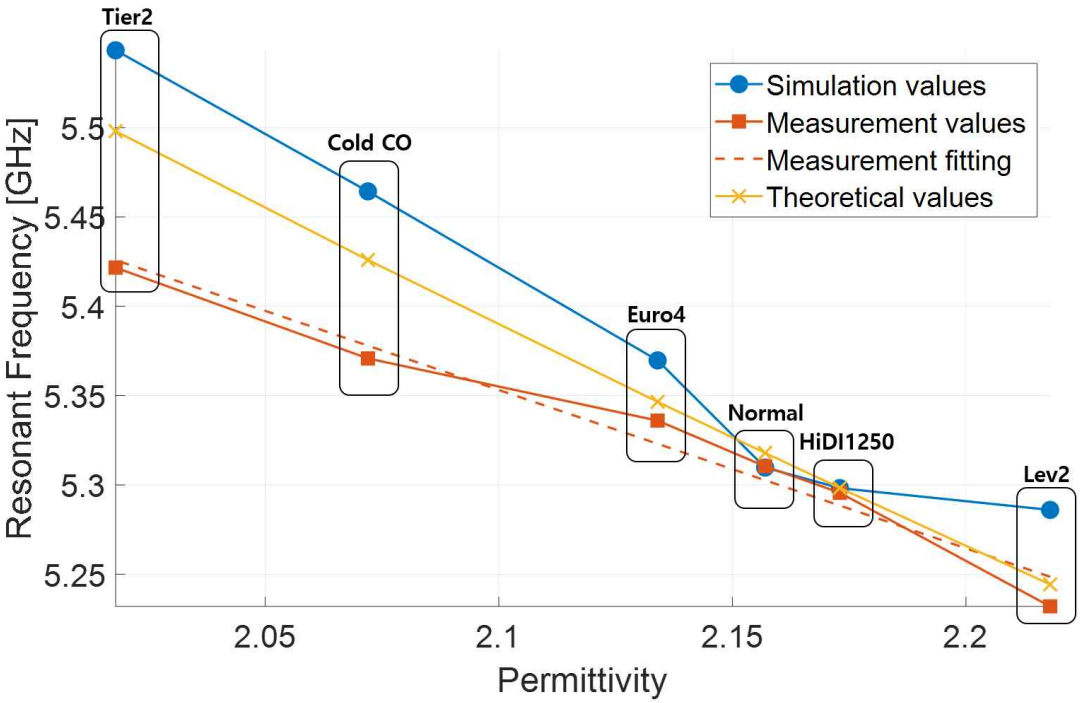

Figure 33. Simulated, experimental and theoretical results of different gasoline samples at room temperature

3.2.2. Experiment at Various Temperatures

When there is a variation in temperature, it also affects the permittivity of the solution, which subsequently changes the resonant frequency of a permittivity-based sensor. For hydrocarbon oils, including gasoline, the change in permittivity with temperature can be calculated following Equation (6), where t is the temperature of the gasoline sample, ϵ_{20} is the relative permittivity at 20℃, and α is the relative permittivity change coefficient that typically ranges from 0.0013 to 0.05% per degree Celsius [35]. For our case, working within the operating frequency of 5 GHz to 6 GHz, increasing the temperature decreases the relative permittivity of normal gasoline ranging from 2.157 to 2.155.

$$\epsilon(t) = \epsilon_{20}(1-\alpha(t-20)) \qquad (6)$$

The experimental setup for evaluating the distinction capability of the proposed sensor under different temperatures is shown in Figure 29. The corresponding experimental schematics to measure the resonant frequency at different temperatures are shown in Figure 30 for the purpose of clarity. In this setup, the sensor is placed in a thermostatic chamber to provide varying temperature conditions using a thermostat. The sensor is connected to a VNA (100 kHz-8.5 GHz, E5063A, KEYSIGHT) via a 50Ω coaxial cable and to a thermostatic bath. The temperature variations were observed from 0℃ to 20℃ with a 5℃ step size increment. To validate the sensing performance of the proposed sensor over repetitive experiments, we measured resonance frequencies and S11 parameters of six samples five times at 5-minute intervals and obtained deviations of 1.73 MHz and 0.286 dB in resonance frequencies and S11 parameters, respectively.

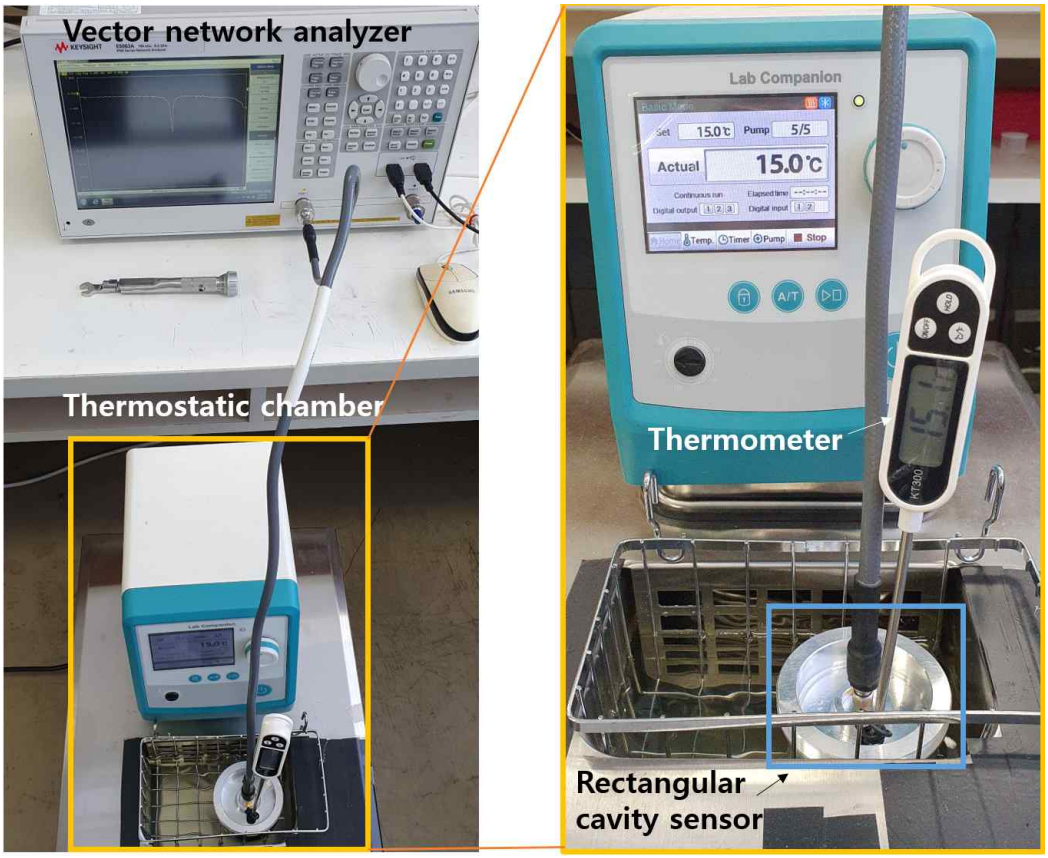

Figure 34. Actual experimental setup for various temperature settings

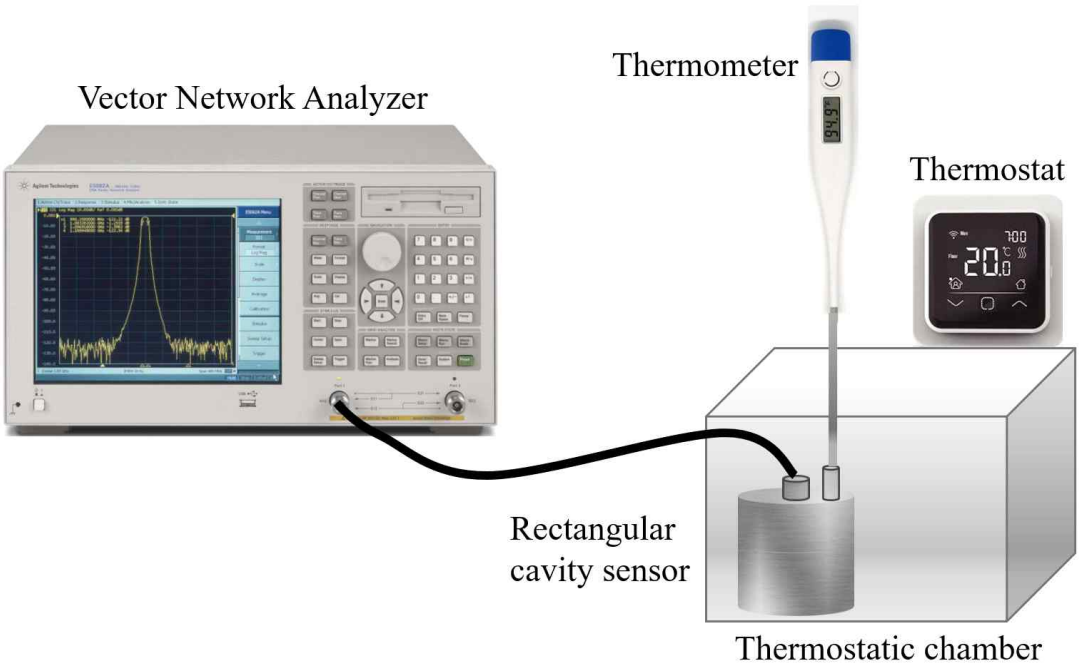

Figure 35. **Schematics of the experimental setup for various temperature settings**

The experimental results are shown in Figure 31, which shows that the sensing property changes are negligible and insensitive to multiple experiments. Note that the S11 parameters of normal gasoline are less than -13 dB. To distinguish normal gasoline from HiDI gasoline regardless of temperature variation, a linear function is derived, as given in Equation (7).

$$f(x_1,x_2) = x_1 + 171.370x_2 - 883.246 < 0 \qquad (7)$$

where x_1 represents the S11 parameter less than -13 dB and x_2 represents the resonance frequency. Figure 32 show the resonance frequency and S11 parameter against temperature as well as the plane corresponding to the function $f(x_1,x_2)$ in Equation (7). Note that the resonance frequencies have a direct relation with temperature; resonance frequencies decline as the temperature decreases. Also, we can notice that the function can detect

normal gasoline from HiDI gasoline with the minimum 4.40 MHz frequency margin and 0.764 dB S11 parameter margin to the closest sample. Since these margins are greater than the average standard deviation of measurements, we can expect the definite and stable distinction property of the proposed sensor.

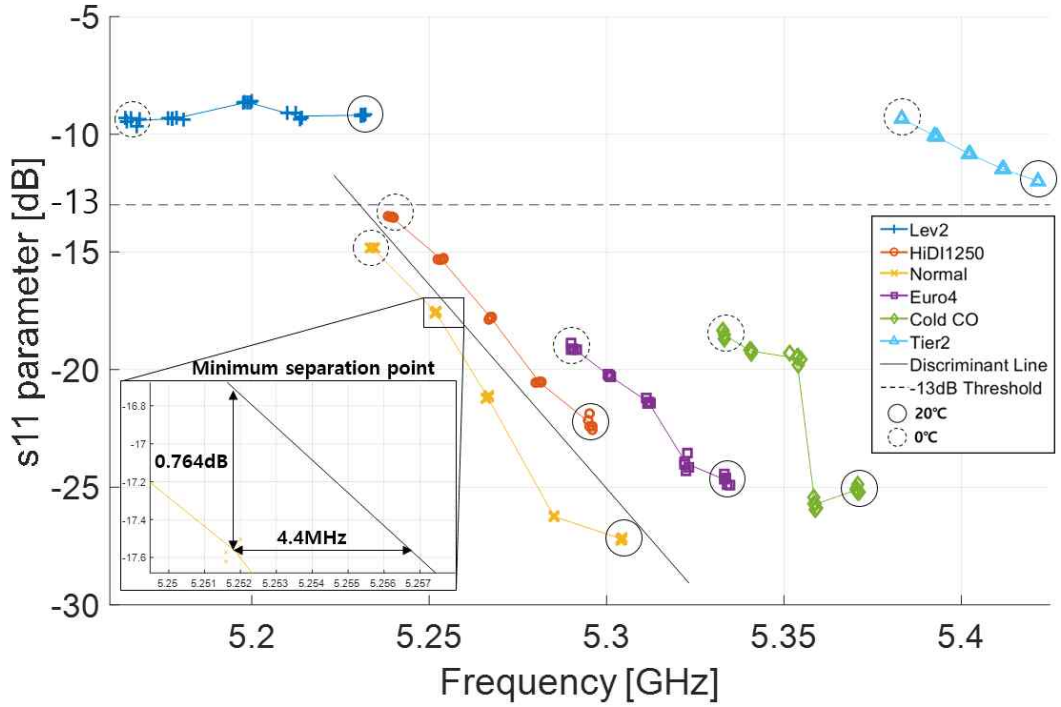

Figure 36. Resonant frequencies and s11 parameters of six gasoline samples at five temperatures obtained by five repetitive experiments

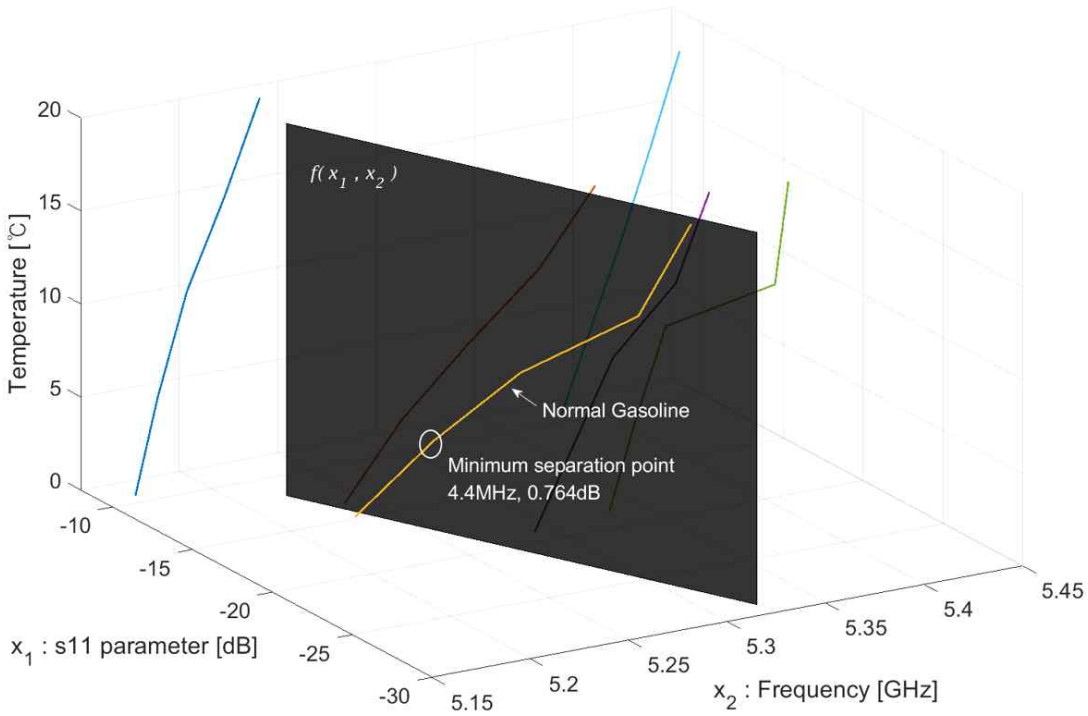

Figure 37. Resonant frequencies and s11 parameters at five temperatures with a decision plane

4. CONCLUSION

Two type cavity sensors are proposed to distinguish between different gasoline samples with minimum permittivity difference of 0.016 at different temperature conditions. The sensing principle of the proposed sensors relies on the change of resonant frequency caused by the change of permittivity of sample inside the cavity sensor. The proposed sensors are designed to have a high Q factor and large frequency separation between gasoline samples. The sensor design parameters are optimized and verified by HFSS simulations. The sensors adopt cavity resonator design which is easy to fabricate and calibrate, has high frequency sensitivity and can be made in compact form.

The presented sensors are fabricated with an enclosed conductive copper cavity and a fixed coupling probe wrapped with Teflon mounted inside the top center of the cavity resonator. The experiments at room temperature confirm effectiveness of gasoline distinction capability. The experimental results are also in agreement with theoretical results which can confirm the accuracy of the proposed sensors. Experiments at various temperatures also show its robust distinction property to temperature variation when the proposed distinction function of resonance frequency and S11 parameter are used. Throughout experiments obtained by changing design parameters and installation position locations, we show reliable, stable and repeatable properties of the proposed sensors. These results prove that the proposed sensors are significantly immune to temperature, position and design variations and thus can be effectively used for gasoline distinction. The proposed sensor design can be applicable to sensor for other liquid detection when the liquid's dielectric property is dominant factor between samles.

REFERENCES

[1] F. Kremer, "Dielectric spectroscopy－yesterday today and tomorrow section 1. Broad band frequency and time domain spectroscopy," J. Non-Crystalline Solids, vol. 305, no. 1, pp. 1-9, 2002.

[2] Mehrotra, P., Chatterjee, B., & Sen, S, "EM-wave biosensors: A review of RF, microwave, mm-wave and optical sensing," Sensors, vol 19, no. 5, 1013, Feb. 2019, doi: 10.3390/s19051013.

[3] R. Raju, G. E. Bridges and S. Bhadra, "Wireless Passive Sensors for Food Quality Monitoring: Improving the Safety of Food Products," IEEE Antennas and Propagation Magazine, vol. 62, no. 5, pp. 76-89, Oct. 2020, doi: 10.1109/MAP.2020.3003216.

[4] C. S. Oon, M. Ateeq, A. Shaw, S. Wylie, A. Al-Shamma'a, and S. N. Kazi, "Detection of the gas - liquid two-phase flow regimes using non-intrusive microwave cylindrical cavity sensor," J. Electromagn. Waves Appl., vol. 30, no. 17, pp. 2241 - 2255, Nov. 2016, doi: 10.1080/09205071.2016.1244019.

[5] M. Hofmann, G. Fischer, R. Weigel and D. Kissinger, "Microwave-Based Noninvasive Concentration Measurements for Biomedical Applications," in IEEE Transactions on Microwave Theory and Techniques, vol. 61, no. 5, pp. 2195-2204, May 2013, doi: 10.1109/TMTT.2013.2250516.

[6] Lee, K., Hassan, A., Lee, C. H., & Bae, J, Microstrip patch sensor for salinity determination. Sensors, vol. 17, no. 12, pp. 2941,Nov. 2017,doi: https://doi.org/10.3390/s17122941.

[7] Zhang, X. Ruan, C. Haq, T. Chen, K. “High-Sensitivity Microwave Sensor for Liquid Characterization Using a Complementary Circular Spiral Resonator,” Sensors, vol. 19, no. 4, pp. 787, Dec. 2019, doi: https://doi.org/10.3390/s19040787.

[8] A. Babajanyan, J. Kim, S. Kim, K. Lee, and B. Friedman, "Sodium chloride sensing by using a near-field microwave microprobe," Appl. Phys. Lett., vol. 89, no. 18, pp. 183504-1 - 183504-3, Oct. 2006, doi: 10.1063/1.2374681.

[9] Memon, M.U. Lim, S. “Microfluidic High-Q Circular Substrate-Integrated Waveguide (SIW) Cavity for Radio Frequency (RF) Chemical Liquid Sensing,” Sensors, vol. 18, no. 1, pp. 143, Jan. 2018, doi: https://doi.org/10.3390/s18010143.

[10] E. L. Chuma, Y. Iano, G. Fontgalland and L. L. Bravo Roger, "Microwave Sensor for Liquid Dielectric Characterization Based on Metamaterial Complementary Split Ring Resonator," IEEE Sensors Journal, vol. 18, no. 24, pp. 9978-9983, 15 Dec.15, 2018, doi: 10.1109/JSEN.2018.2872859.

[11] P. Vélez, L. Su, K. Grenier, J. Mata-Contreras, D. Dubuc and F. Martín, "Microwave Microfluidic Sensor Based on a Microstrip Splitter/Combiner Configuration and Split Ring Resonators (SRRs) for Dielectric

Characterization of Liquids," in IEEE Sensors Journal, vol. 17, no. 20, pp. 6589-6598, 15 Oct.15, 2017, doi: 10.1109/JSEN.2017.2747764.

[12] S. Jorgensen et al., "Evaluation of New Volatility Indices for Modern Fuels," SAE Technical Paper., 1999-01-1549, May. 1999, doi: https://doi.org/10.4271/1999-01-1549.

[13] B. Evans et al., "New gasoline volatility indices," Automot. Eng., pp. 175 - 176, May 2000.

[14] Lambert, D., Harrington, C., Kerr, R., Lee, H. et al., Fuel Driveability Index Sensor, SAE Technical Paper 2003-01-3238, 2003

[15] Ferguson, Todd J., Joseph R. Griffin, and Francis De Blauwe. High DI fuel detection via exhaust gas temperature measurement for ULEV. No. 2000-01-0893. SAE Technical Paper, 2000.

[16] Guo, Hongfu, Lu Yao, and Fen Huang. A cylindrical cavity sensor for liquid water content measurement. Sensors and Actuators A: Physical 238 2016: 133-139.

[17] K. Saeed, R. Pollard, I. C. Hunter, Substrate integrated waveguide cavity resonator for complex permittivity characterization of materials, Trans. Microw. Theory Tech., vol. 56, no. 10, pp. 2340-2347, Oct. 2008

[18] Cuenca, Jerome A., Daniel R. Slocombe, and Adrian Porch. Temperature correction for cylindrical cavity perturbation measurements. IEEE Transactions on Microwave Theory and Techniques 65, no. 6 2017: 2153-2161.

[19] Xiang Li, Yan Jiang. Design of a Cylindrical Cavity Resonator for Measurements of Electrical Properties of Dielectric Materials. Master Thesis in Electronics/Telecommunications, 2010

[20] . Zhao zong Meng, Zhipeng Wu and John Gray. Microwave sensor technologies for food evaluation and analysis: Methods, challenges and solutions. Transactions of the Institute of Measurement and Control 40 no. 12 2018: 3433-3448

[21] Meitzler, Allen H., and George S. Saloka. Two alternative, dielectric-effect, flexible-fuel sensors. SAE transactions, 1992: 1455-1466.

[22] Oon, Cheen Sean, Muhammad Ateeq, Andy Shaw, Stephen Wylie, Ahmed Al-Shamma'a, and Salim Newaz Kazi. Detection of the gas - liquid two-phase flow regimes using non-intrusive microwave cylindrical cavity sensor. Journal of Electromagnetic Waves and applications 30, no. 17 2016: 2241-2255

[23] Oon, C. S., M. Ateeq, A. Shaw, A. Al-Shamma'a, S. N. Kazi, and A. Badarudin. Experimental study on a feasibility of using electromagnetic wave cylindrical cavity sensor to monitor the percentage of water fraction in a two phase system. Sensors and Actuators A: Physical 245 2016: 140-149.

[24] Zinal, Sherko, and Georg Boeck. Complex permittivity measurements using TE/sub 11p/modes in circular cylindrical cavities. IEEE transactions on microwave theory and techniques 53, no. 6 2005: 1870-1874.

[25] Jensen, Erk. Rf cavity design. arXiv preprint arXiv:1601.05230 2016.

[26] A. Mason, B. Abdullah, M. Muradov, O. Korostynska, A. Al-Shamma'a, S.G. Bjarnadottir, K. Lunde, O. Alvseike. Theoretical basis and application for measuring pork loin drip loss using microwave spectroscopy, Sensors 16 2016: 1 - 13

[27] Jim Frusti, Chrysler, California LEVIII Certification Fuel Gasoline. ARB Public Workshop, El Monte, Calif - Alliance Fuels Group Comments, delivered July 19, 2011

[28] Wikipedia contributors. European emission standards [Internet]. Wikipedia, The Free Encyclopedia; 2019 Aug 15.

[29] Dielectric Constants of Common Materials, In KAB Electro Acoustics.

[30] Carey AA, Hayzen AJ. Machinery lubrication - The Dielectric Constant and Oil Analysis. Emerson Process Management, August 2013

[31] Bezman, Richard D., Edward F. Casassa, and Robert L. Kay. The temperature dependence of the dielectric constants of alkanols. Journal of molecular liquids 73 1997: 397-402

[32] A. Webb, "Cavity- and waveguide-resonators in electron paramagnetic resonance, nuclear magnetic resonance, and magnetic resonance imaging," Progress Nucl. Magn. Resonance Spectroscopy, vol. 83, pp. 1 - 20, Nov. 2014, doi: 10.1016/j.pnmrs.2014.09.003.

[33] B.-H. Liu, D. C. Chang, and M. T. Ma, "Eigenmodes and the composite quality factor of a reverberating chamber," no. 1066, 1983.

[34] M. T. Sebastian, M. A. S. Silva, and A. S. B. Sombra, "Measurement of microwave dielectric properties and factors affecting them," in Microw. Mater. Appl. 2V Set, M. T. Sebastian, H. Jantunen, and R. Ubic, Eds. Chichester, UK: John Wiley & Sons, Ltd, 2017, p. 1e51.

[35] A. A. Carey and A. J. Hayzen, "Machinery Lubrication－The Relative permittivity and Oil Analysis. Emerson Process Management," 2013. http://www.Machinerylubrication.com/Read/226/dielectric-constant-oil-analysis. Accessed on: Aug. 20, 2020.